Presentation at DESY, Hamburg, Germany, Feb. 05, 2008

Ground Penetrating Radar for the Detection of Buried Nonmetallic Anti-Personnel Landmines

Dipl.-Wirtsch.-Ing. Alexander Teggatz

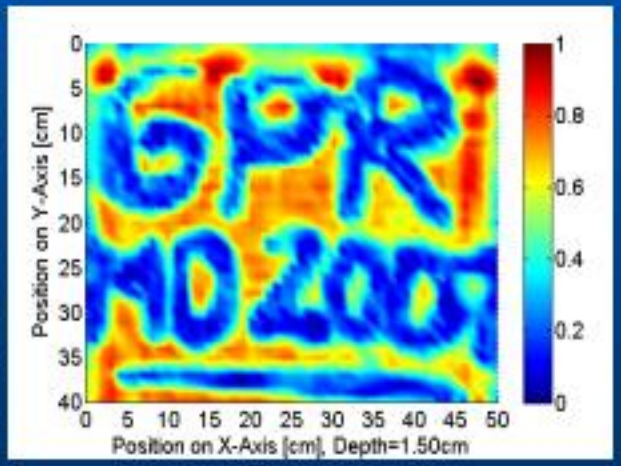

Otto-von-Guericke-University of Magdeburg, FEIT
Electronics, Signal Processing and Communications
alexander.teggatz@e-technik.uni-magdeburg.de

Outline

- Introduction
- 3D Field Simulation of a GPR
- SAR Focusing Techniques for GPR
- Laboratory GPR Measurements
- Outdoor GPR Measurements
- Conclusion

Outline

- Introduction
- 3D Field Simulation of a GPR
- SAR Focusing Techniques for GPR
- Laboratory GPR Measurements
- Outdoor GPR Measurements
- Conclusion

Global Landmine Crisis

- 1997 Ottawa Convention to ban landmines, 155 countries but not USA, Russia, China…
- 340 types of Anti-Personnel Mines (APM)
- 100 million APM in over 70 countries
- 2000 persons killed, wounded monthly
- Cost of production 3$ - 30$ / APM
- Cost of removal 300$ - 1000$ / APM
- One accident per 1000 APM removed

Ground Penetrating Radar

- Problem: Detection of buried Anti-Personnel Landmines which are made without any metal
- Promising: Ground Penetrating Radar (GPR)
  - Idea originates from geological techniques
  - Record the reflection of the transmitted signal
  - Detection of hidden dielectric discontinuities
- PhD-Thesis: Investigate the imaging capabilities of GPR and define all important GPR parameter?

Resolution of a GPR

- Vertical Resolution („up-down“ direction)
  - Determined by the bandwidth of the GPR
  - Optimization: Increase the radar bandwidth
  - Limitation: Low pass behavior of the soil
- Lateral Resolution („horizontal“ direction)
  - Determined by the diameter of Fresnel zone
  - Limitation: Wavelength at lowest frequency
  - Trade-off with the vertical system resolution

Illustration of GPR Data

- Common perspectives for visualization of GPR-data:
- two-dimensional plots…
  A-Scan (one single position)
  B-Scan (one vertical layer)
  C-Scan (one horizontal layer)
- …or three-dimensional plot with proper threshold value

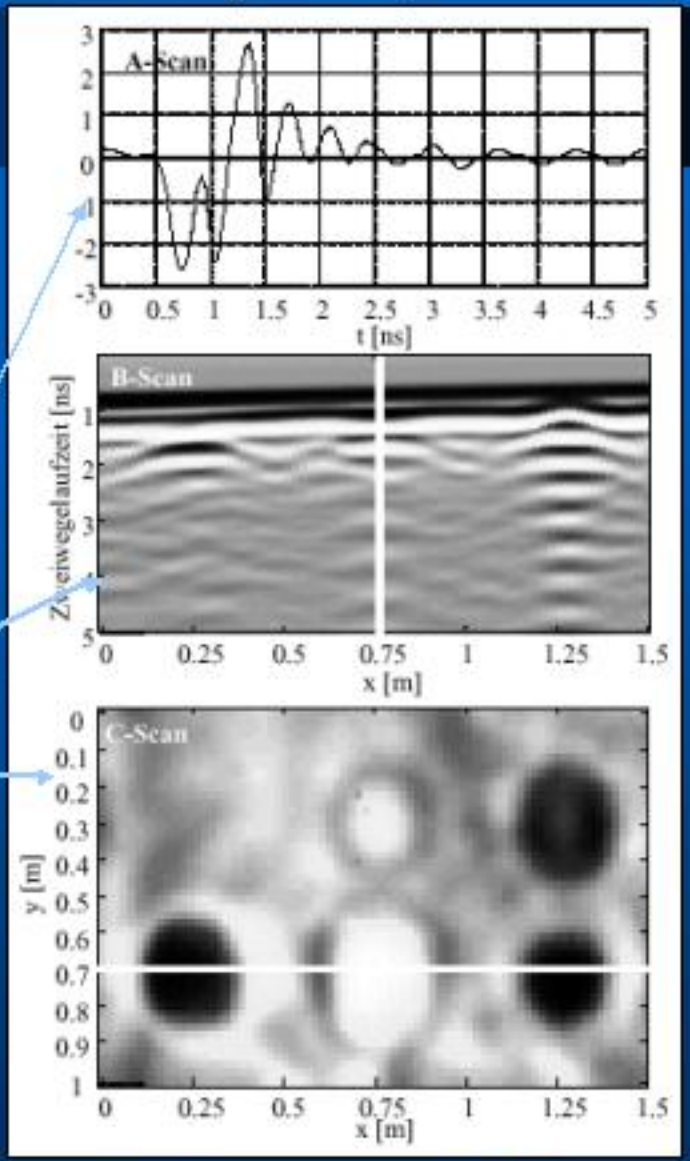

Outline

- Introduction
- 3D Field Simulation of a GPR
- SAR Focusing Techniques for GPR
- Laboratory GPR Measurements
- Outdoor GPR Measurements
- Conclusion

3D Field Simulation of a GPR

- Antenna optimization in the context of GPR
- Support for a systematical design approach
- Datasets with exactly defined characteristics

WHY?

- CST Microwave Studio (3D EM FIT Solver)
- GPR problem can be customized by the user
- Simulation of all antenna position on x-y-grid
- Script-controlled automation of the simulation

HOW?

3D Field Simulation of a GPR cont.

- Full functionality of CST Studio Suite is open for a Visual Basic for Applications (VBA) script control
- VBA objects can be found in CST documentation
- VBA script either directly in CST Studio Suite or from an external application (Mathworks Matlab)
- For the case of an external control:
  - ActiveX server connection to all VBA functions
  - VBA functionality accessible by remote control

3D Field Simulation of a GPR cont.

- Investigation and comparison of several different antenna concepts for subsurface radar applications


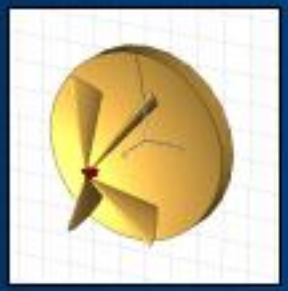
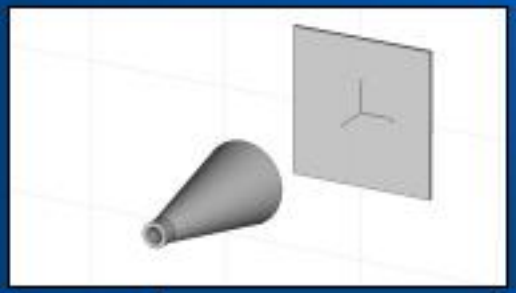





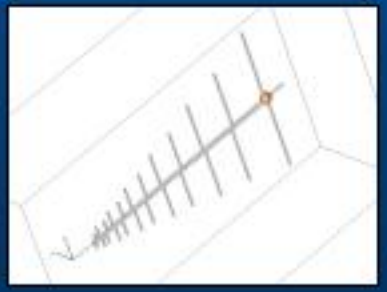


3D Field Simulation of a GPR cont.

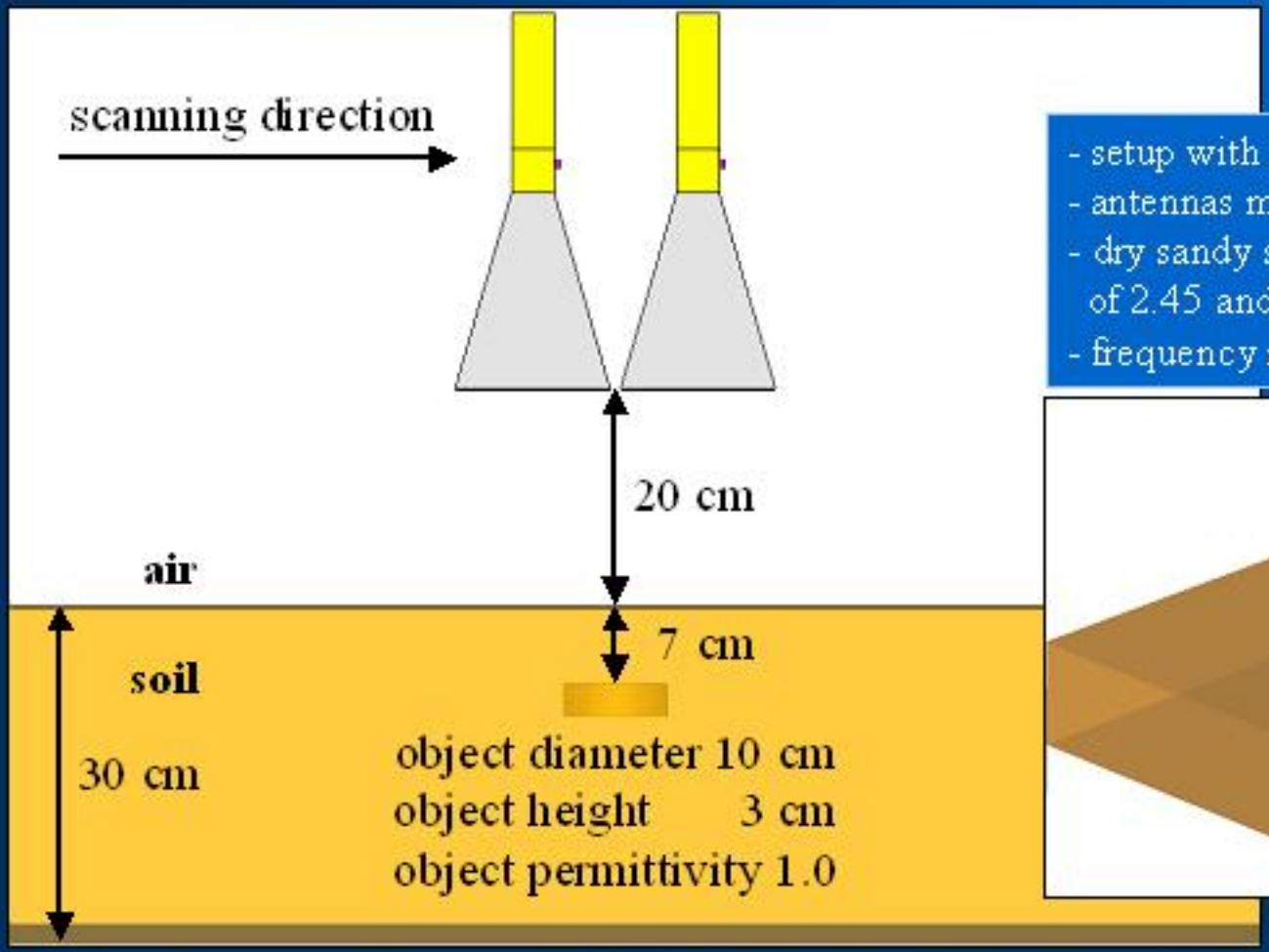

- setup with 2 TEM horn antennas
- antennas moved in fixed distance
- dry sandy soil with a permittivity of 2.45 and a loss tangent of 0.016
- frequency range 1 GHz – 10 GHz

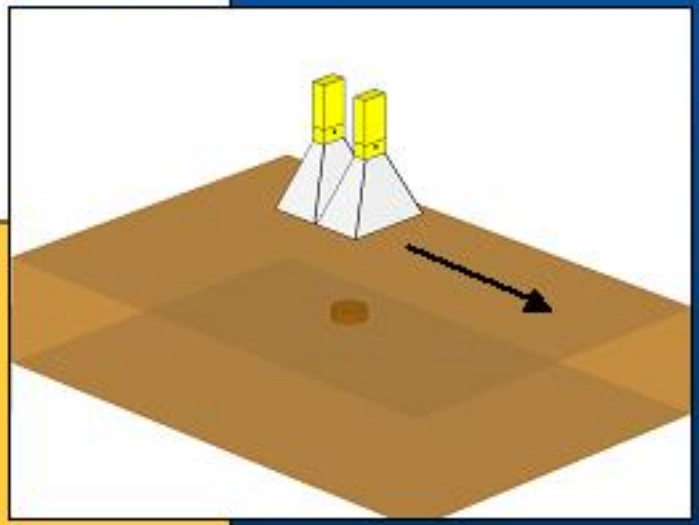

3D Field Simulation of a GPR cont.

- Two antenna case with S_{21} vs. single antenna results with S_{22}
- Post processing: Carrier removal and background subtraction

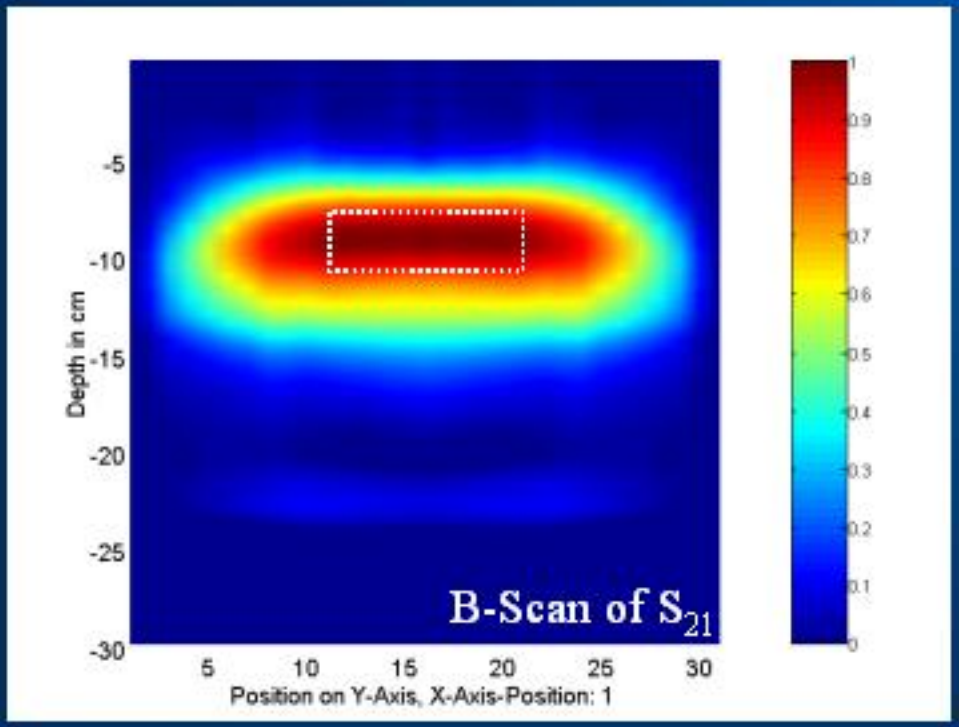

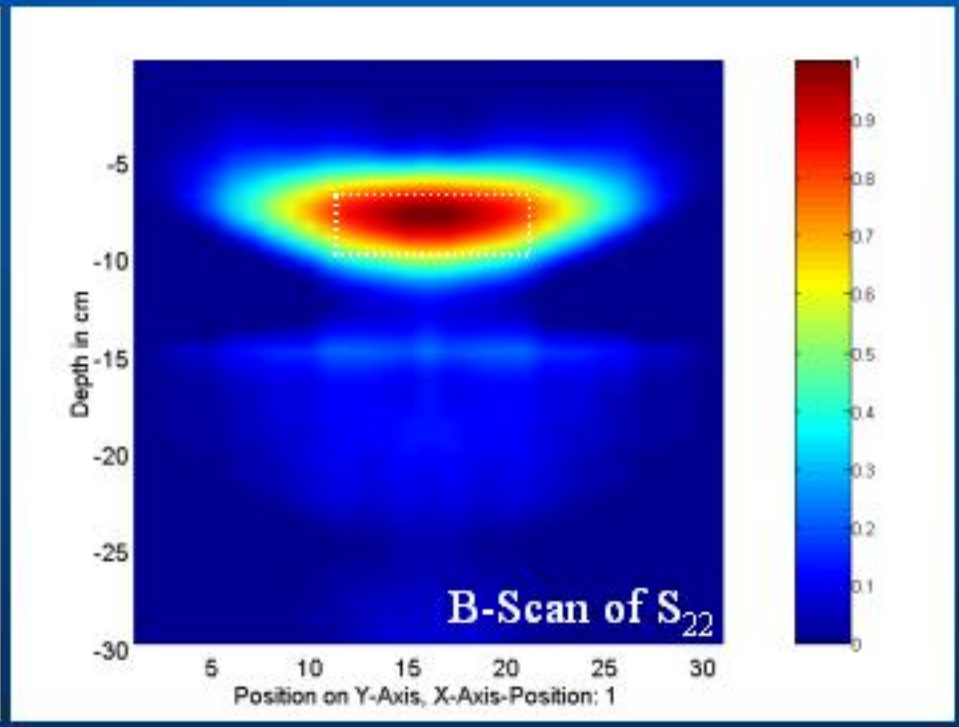

Outline

- Introduction
- 3D Field Simulation of a GPR
- SAR Focusing Techniques for GPR
- Laboratory GPR Measurements
- Outdoor GPR Measurements
- Conclusion

Synthetic Aperture Radar

- Idea: combine series of observations as if they had been made simultaneously from a very large antenna
- Computational fast SAR method for 3D subsurface focusing by 2D processing (Yakubov, Omar, et al.)
- Implementation of the SAR method:
  - Assumption of 1st Order Born approximation
  - Focusing on 2D plane at the surface of the soil
  - Focused beam remains concentrated in the soil

Synthetic Aperture Radar cont.

GPR Measurement
Measurement of S_{11} at different positions of the GPR antenna.

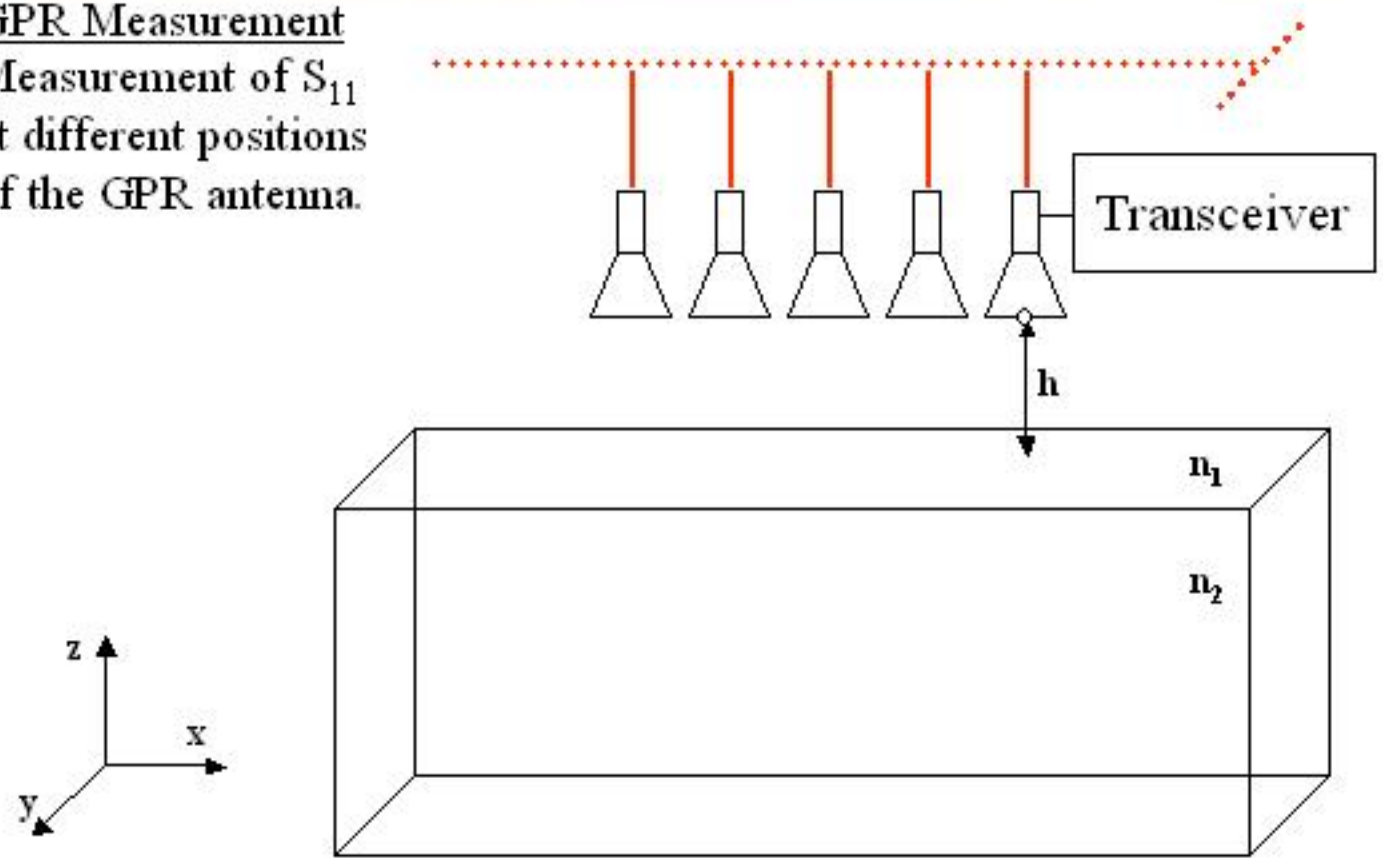

Synthetic Aperture Radar cont.

SAR Processing

Calculate distance in the x- and y-direction between phase center and the focus point F.

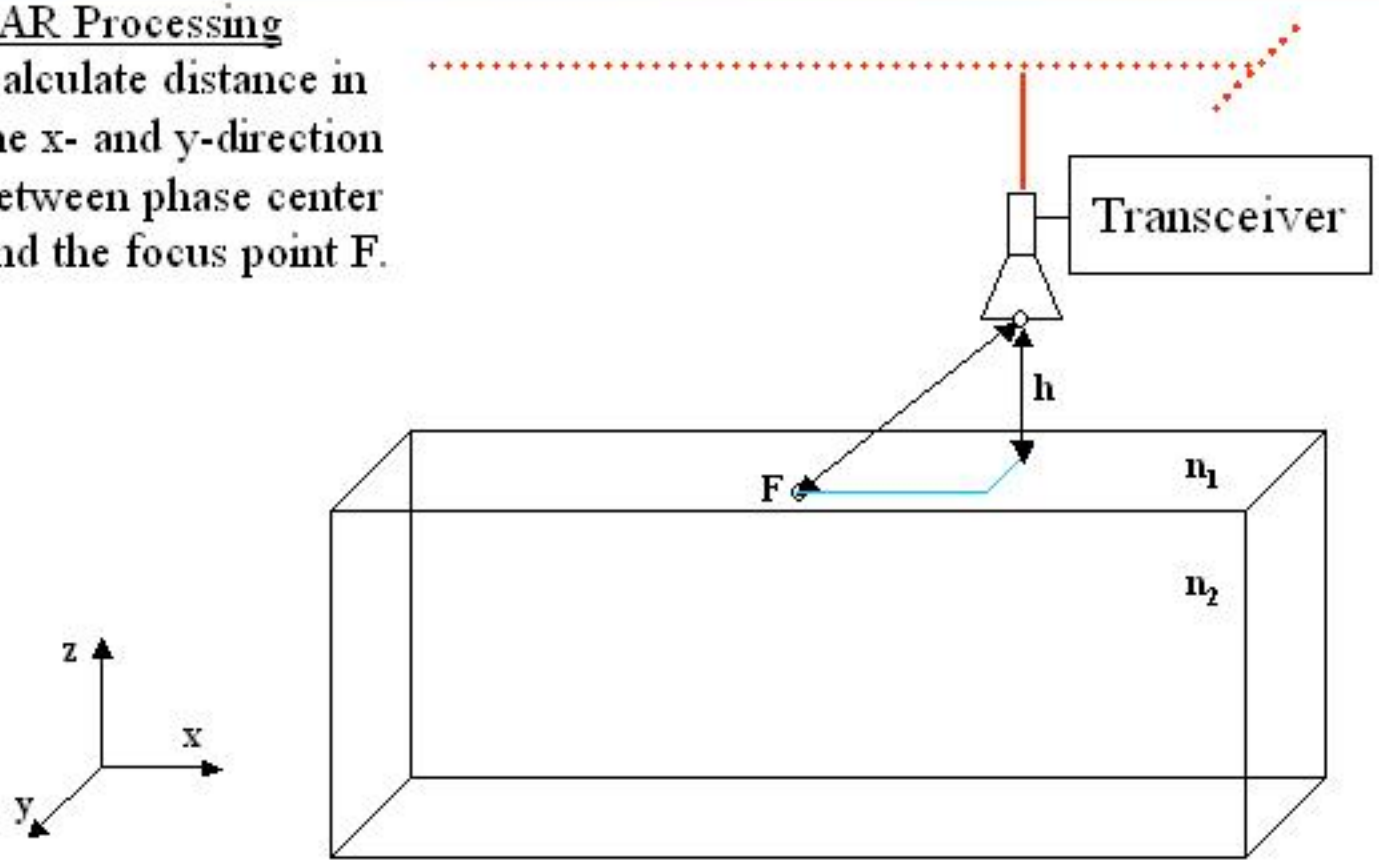

Synthetic Aperture Radar cont.

Measured data

$$S(x, y, f)$$

SAR Focusing (Phase Correction)

$$U(x_F, y_F, f) = \int_x \int_y S(x, y, f) H(x - x_F, y - y_F) dx_F dy_F$$

$$H(x, y) = \exp(-j2k(\sqrt{x^2 + y^2 + h^2}))$$

Inverse Fourier Transformation

$$\tilde{U}(x_F, y_F, t) = \int_f U(x_F, y_F, f) \exp(-j2\pi f) df$$

Reconstructed distribution

$$\Delta\varepsilon(x_F, y_F, z) \approx \tilde{U}(x_F, y_F, t)$$

Evaluation of the Focusing

- How to determine the quality of the focusing?
  - Choose a single focus point on or in the soil.
  - Apply the phase correction for every antenna.
  - Compare the results of different array setups.

- Parameter that effect the focusing:
  - Number of array elements (m,n)
  - Distance between the elements

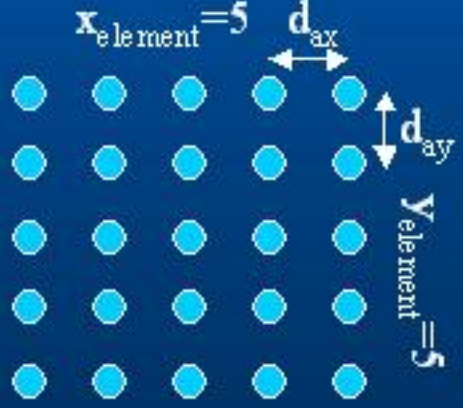

Analytical Dipole Array cont.

- Calculation of E- and H-field below dipol array
- Orientation of elementary dipole above the soil:

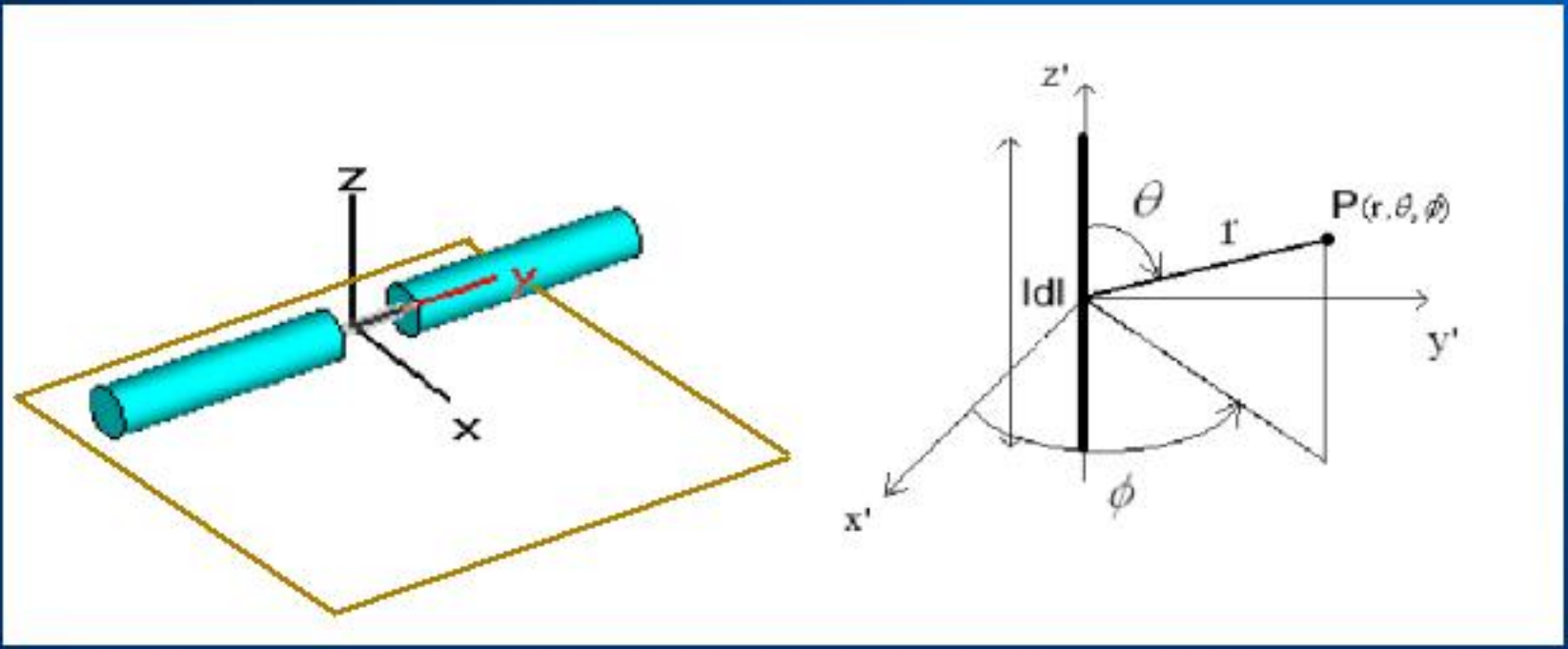

Analytical Dipole Array cont.

- Determine r, θ and φ for every surface point.
- Calculate all the spherical field components of a dipole without a farfield approximation!

$$
\begin{aligned}
E_\phi &= H_r = H_\theta = 0 \\
E_r &= 2kZ_0 I dl e^{-jkr} \cdot \frac{1}{4\pi r} \cdot \cos\theta \cdot \left(\frac{1}{kr} - j\frac{1}{(kr)^2} \right) \\
E_\theta &= jkZ_0 I dl e^{-jkr} \cdot \frac{1}{4\pi r} \cdot \sin\theta \cdot \left(1 - j\frac{1}{kr} - \frac{1}{(kr)^2} \right) \\
H_\phi &= jkI dl e^{-jkr} \cdot \frac{1}{4\pi r} \cdot \sin\theta \cdot \left(1 - j\frac{1}{kr} \right)
\end{aligned}
$$

Analytical Dipole Array cont.

- Computational efficient calculation of the E-/H-field for an array of elementary dipole antennas:
- Calculate E- / H-field of a single dipole element.
- Utilize the field results for every array position.

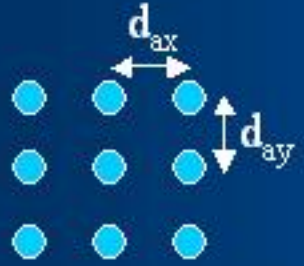

dipole array (3*3 elements)

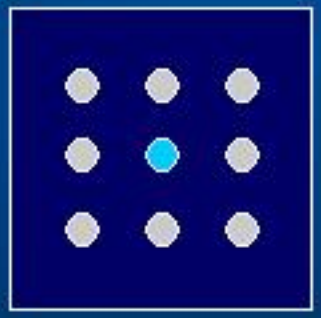

E- and H-field of single dipole

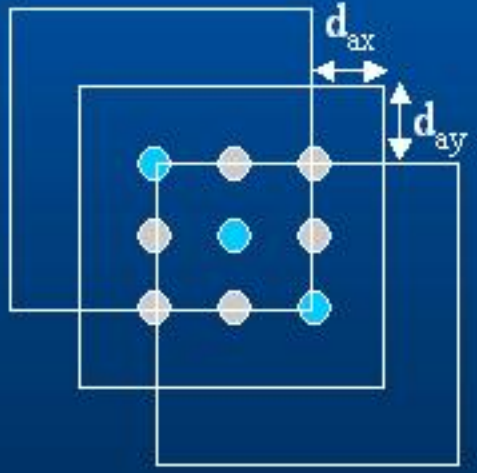

Analytical Dipole Array cont.

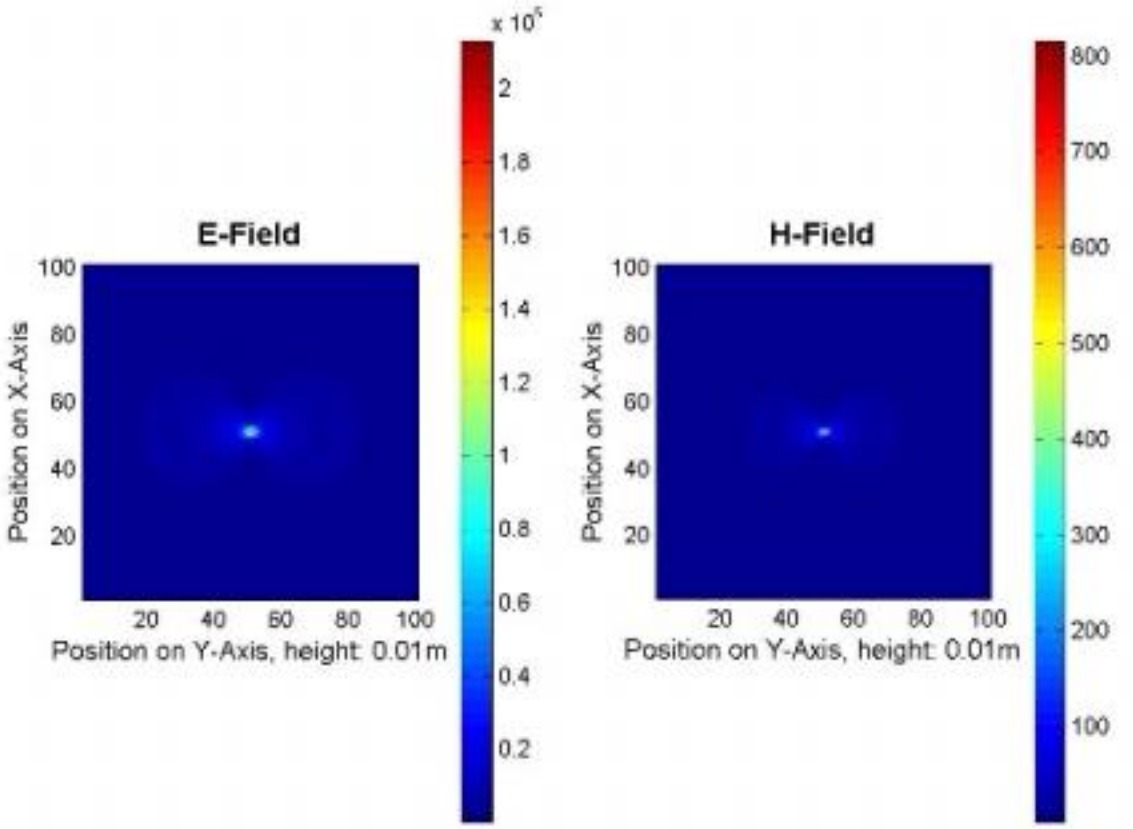

$$E-Field = \sqrt{0.5\cdot\left(|E_x|^2+|E_y|^2+|E_z|^2\right)}$$

$$H-Field = \sqrt{0.5\cdot\left(|H_x|^2+|H_y|^2+|H_z|^2\right)}$$

f_{op}=5 GHz

$x_{element}$=1

$y_{element}$=1

Analytical Dipole Array cont.

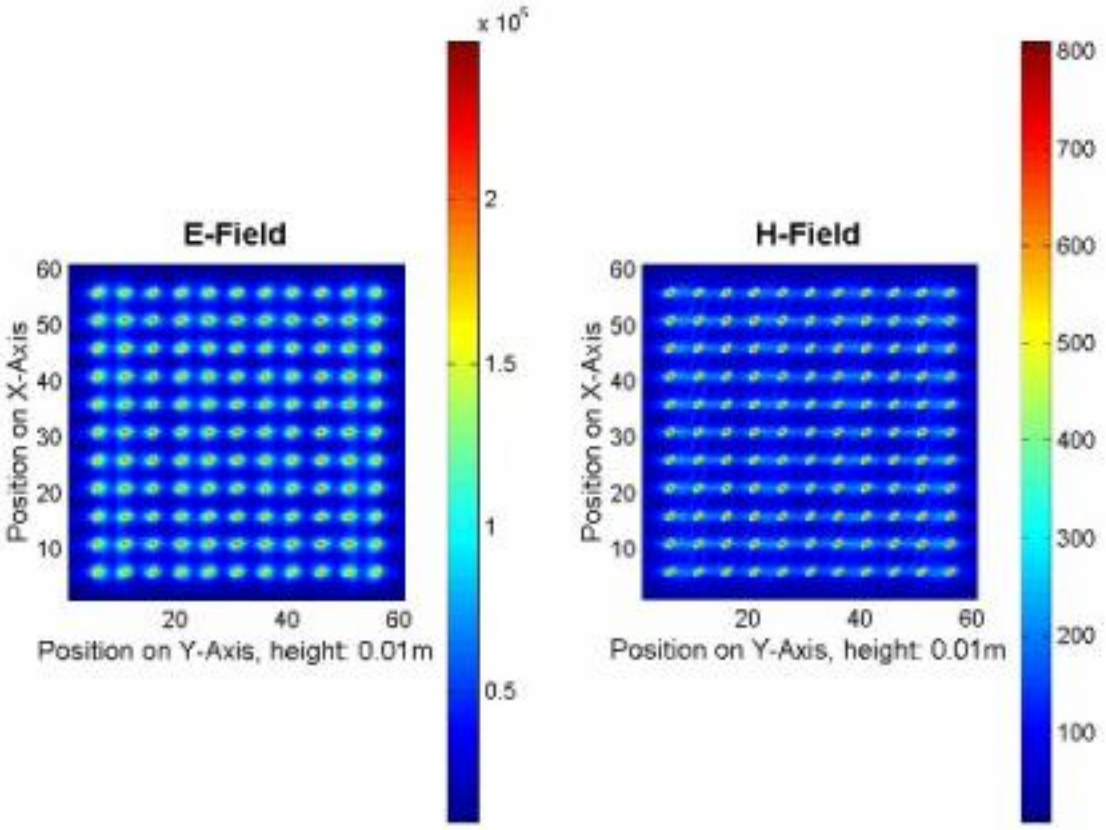

$$E-Field = \sqrt{0.5\cdot\left(|E_x|^2+|E_y|^2+|E_z|^2\right)}$$

$$H-Field = \sqrt{0.5\cdot\left(|H_x|^2+|H_y|^2+|H_z|^2\right)}$$

f_{op}=5 GHz
$x_{element}$=11
$y_{element}$=11
d_{ax}=10 cm
d_{ay}=10 cm

Analytical Dipole Array cont.

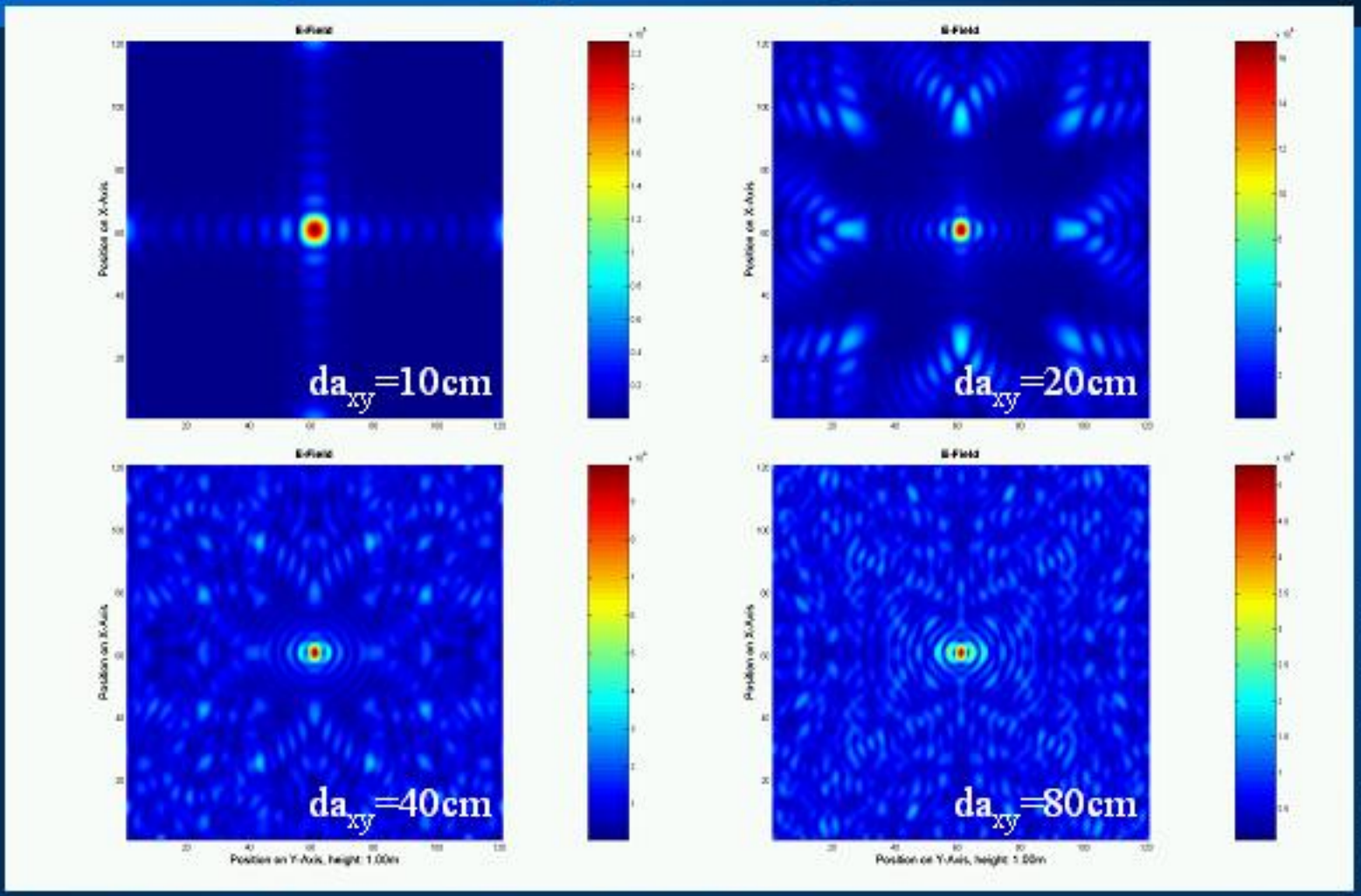

with SAR

f_{op}=5 GHz

$x_{element}$=11

$y_{element}$=11

h_{focus}=1 m

Analytical Dipole Array cont.

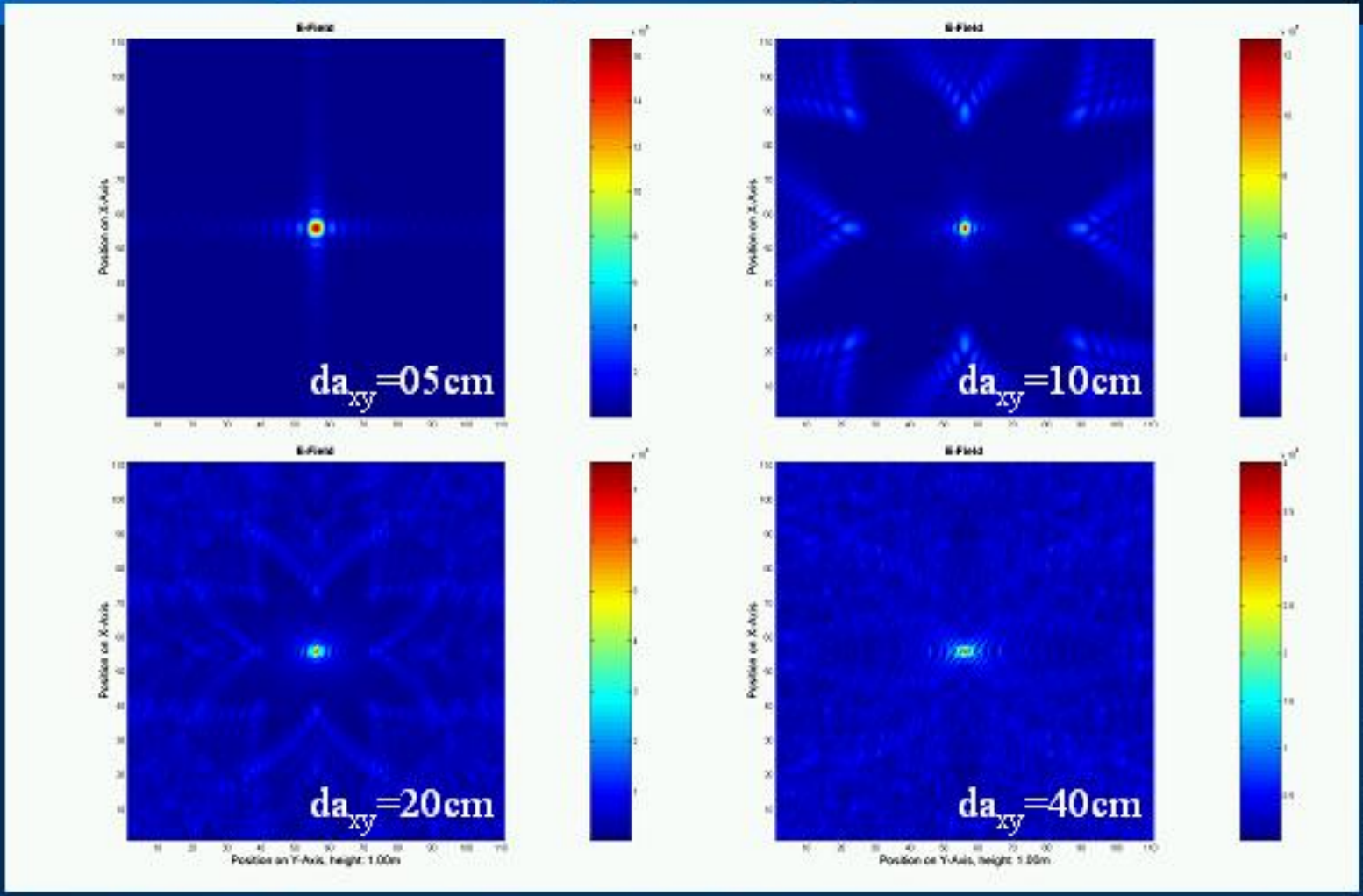

with SAR

f_{op}=10 GHz

$x_{element}$=21

$y_{element}$=21

h_{focus}=1 m

Numerical Field Simulation

- Evaluation of the SAR focusing inside the soil
- Prove the assumption of a narrow energy beam
- Numerical SAR simulation technique:
  - Uses the 3D EM field simulation of a GPR
  - Modified TEM double-ridged horn antenna
  - Homogeneous soil, permittivity of dry sand
  - Monitor E- and H-field for different depths

Numerical Field Simulation cont.

MWS Simulation
OPTERON, 8 GB

2D E-Field Monitors
2D H-Field Monitors
from surface to 0.5m

Modified TEM
Horn Antenna

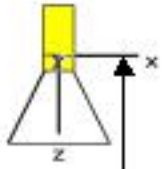

100 cm

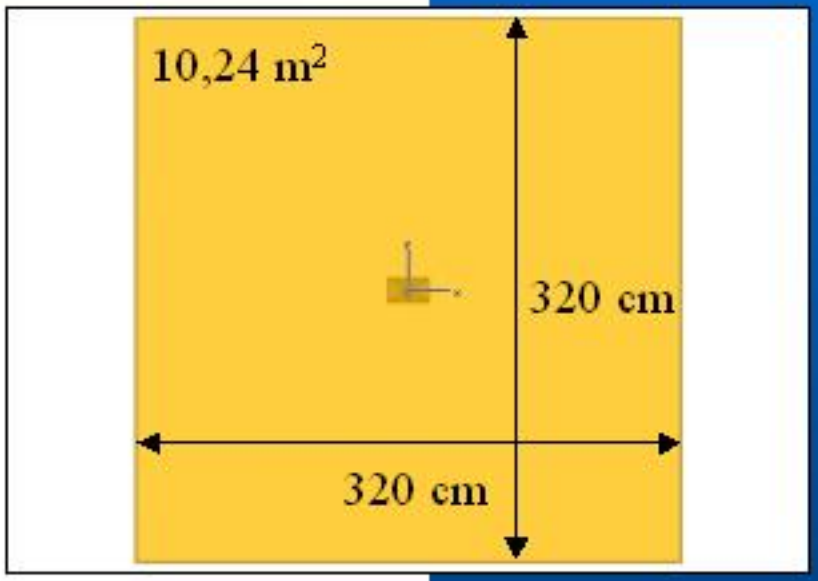

homogeneous soil
with e_r=2.45 and a
loss tangent of 0.01

50 cm

320 cm

Numerical Field Simulation cont.

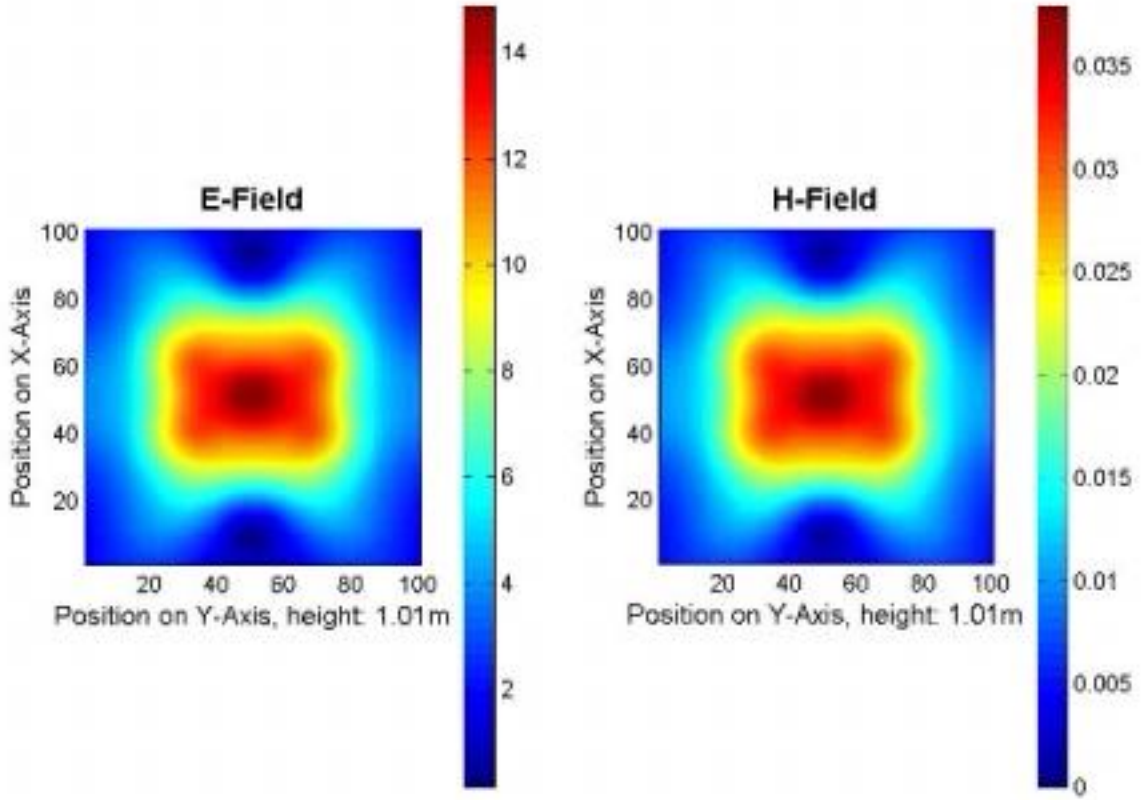

$$E-Field = \sqrt{0.5\cdot\left(|E_x|^2+|E_y|^2+|E_z|^2\right)}$$

$$H-Field = \sqrt{0.5\cdot\left(|H_x|^2+|H_y|^2+|H_z|^2\right)}$$

f_{op}=5 GHz

$x_{element}$=1

$y_{element}$=1

Numerical Field Simulation cont.

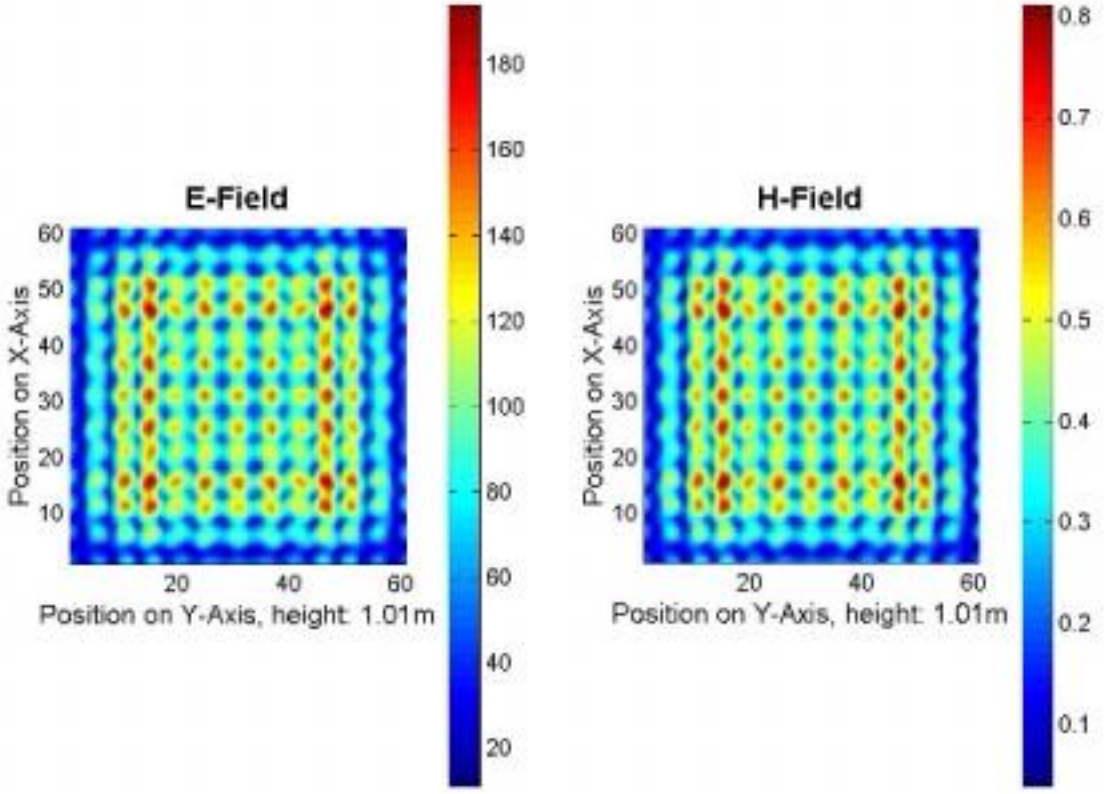

$$E - Field = \sqrt{0.5 \cdot (|E_x|^2 + |E_y|^2 + |E_z|^2)}$$

$$H - Field = \sqrt{0.5 \cdot (|H_x|^2 + |H_y|^2 + |H_z|^2)}$$

f_{op}=5 GHz
$x_{element}$=11
$y_{element}$=11
d_{ax}=10 cm
d_{ay}=10 cm

Numerical Field Simulation cont.

- TEM Horn Array: 11x11, da_{xy}=10 cm, $f_{operation}$=5 GHz
  h_{focus}=100 cm, depth=101 – 150 cm

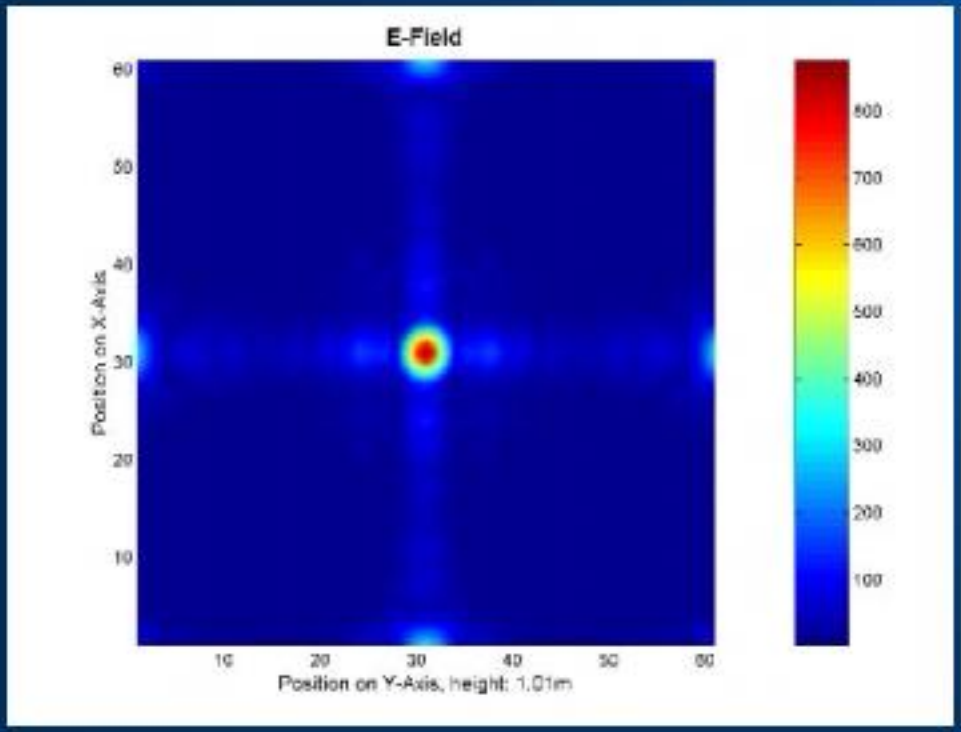

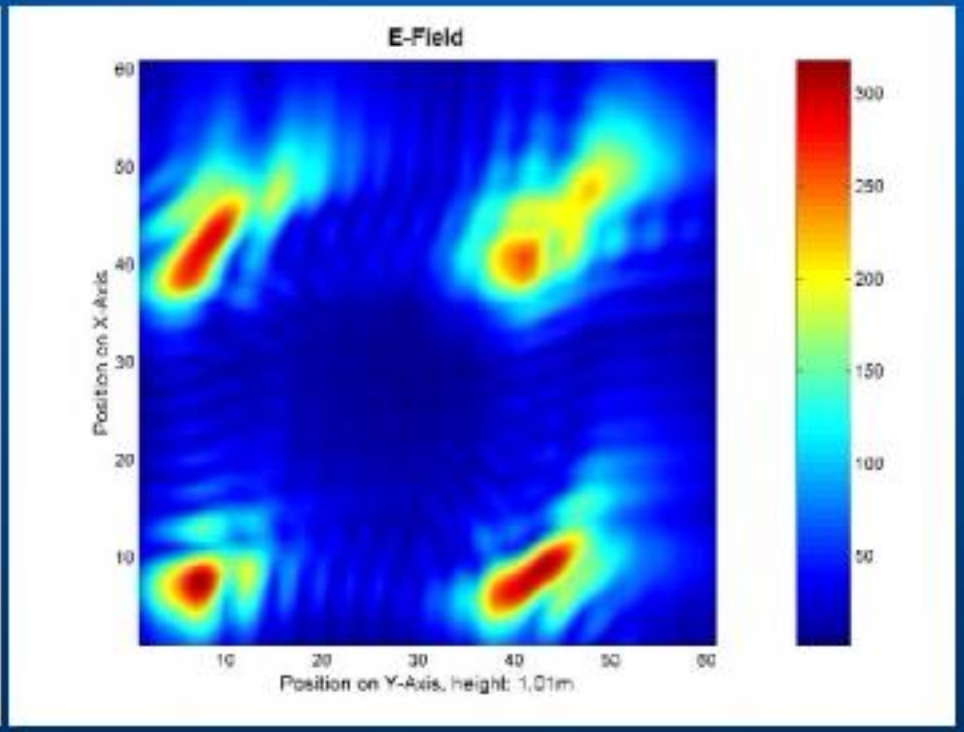

Numerical Field Simulation cont.

- Left: 21x21 array, da_{xy}=1 cm, $f_{op.}$=5 GHz, focus at (21,11)
- Right: 21x21 array, da_{xy}=1 cm, $f_{op.}$=5 GHz, focus at (21,1)

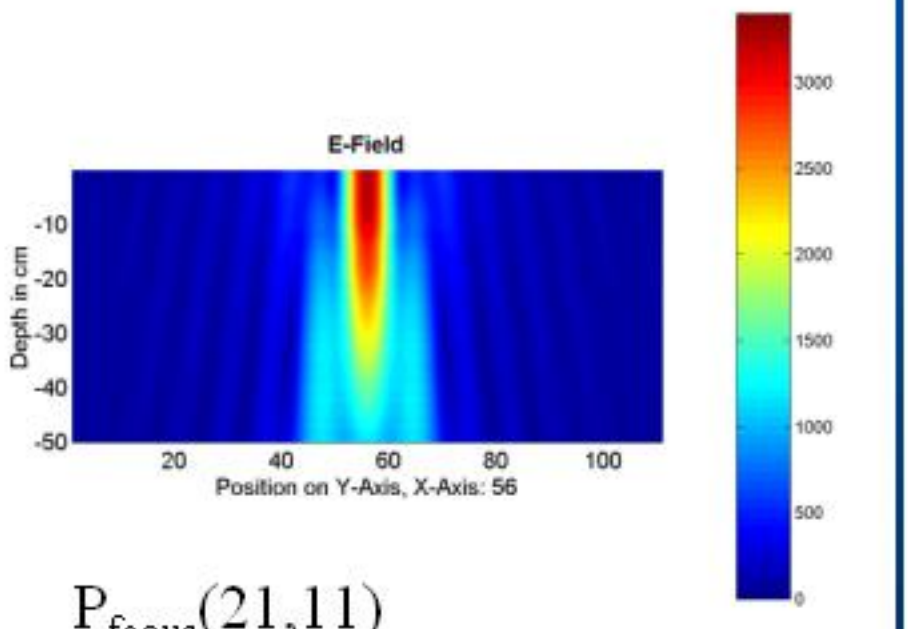

$P_{focus}(21,11)$

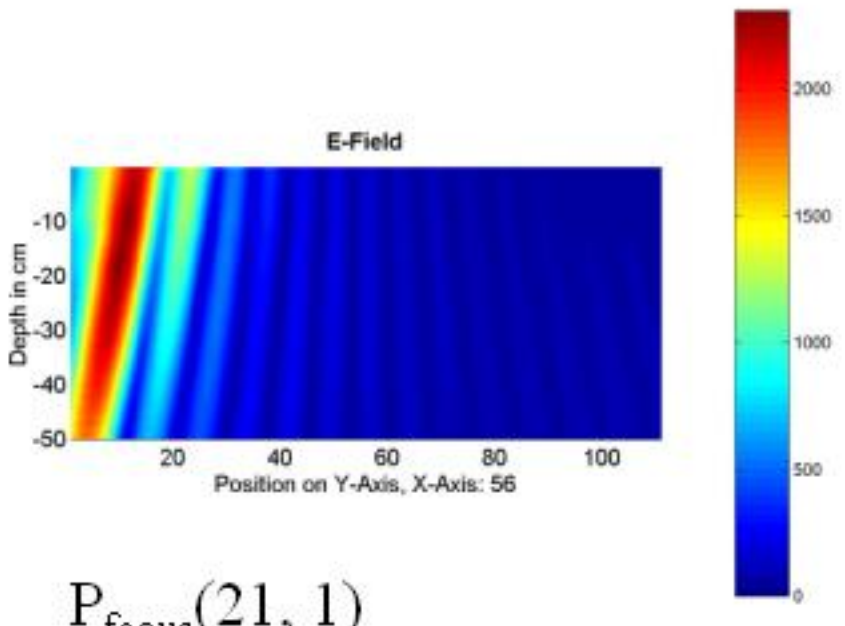

$P_{focus}(21, 1)$

Outline

- Introduction
- 3D Field Simulation of a GPR
- SAR Focusing Techniques for GPR
- Laboratory GPR Measurements
- Outdoor GPR Measurements
- Conclusion

Laboratory GPR Measurements

- Linear stepper motors move VNA + antenna along 2 axis
- Complete GPR scanning procedure is controlled by one PC

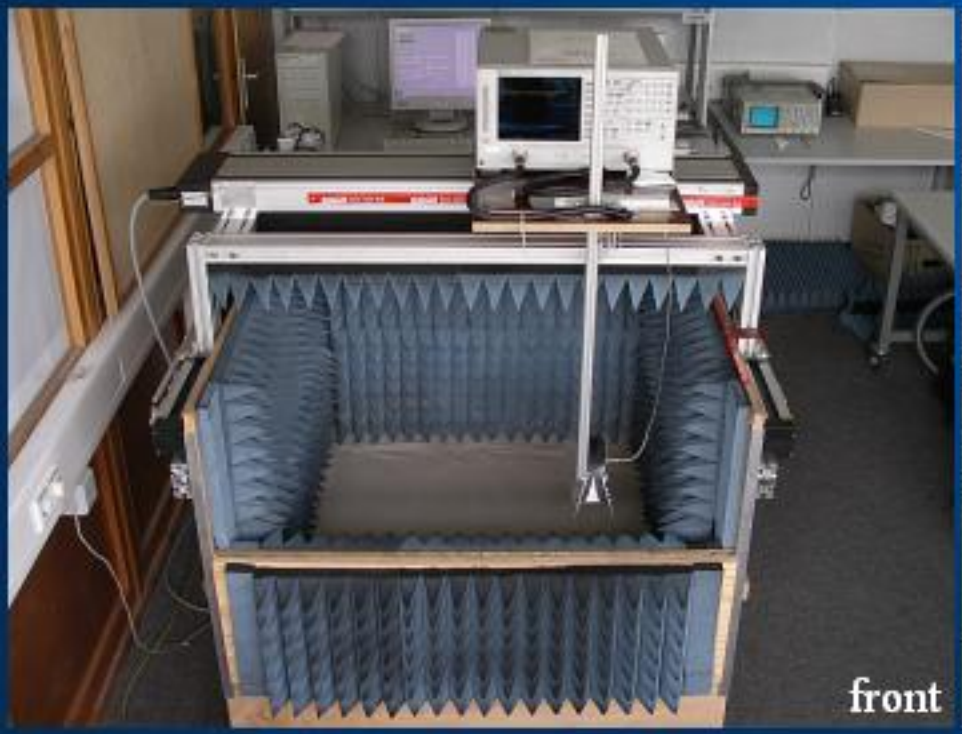

Laboratory GPR Measurements cont.

- Measurement I: TEM double-ridged horn, 30 cm above soil
- VNA SFCW measurement, frequency range 3 GHz - 10 GHz

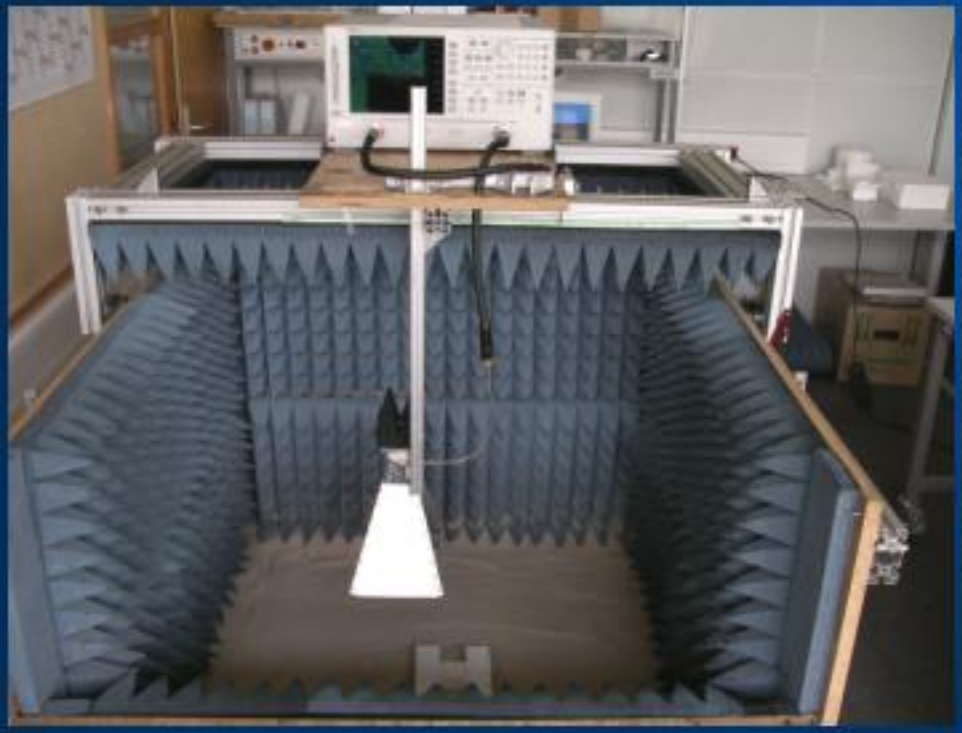

Laboratory GPR Measurements cont.

- Object 1: 3-stepped foam, height 5 cm, in a depth of 7 cm
- Object 2: H-shaped foam, height 5 cm, in a depth of 7 cm

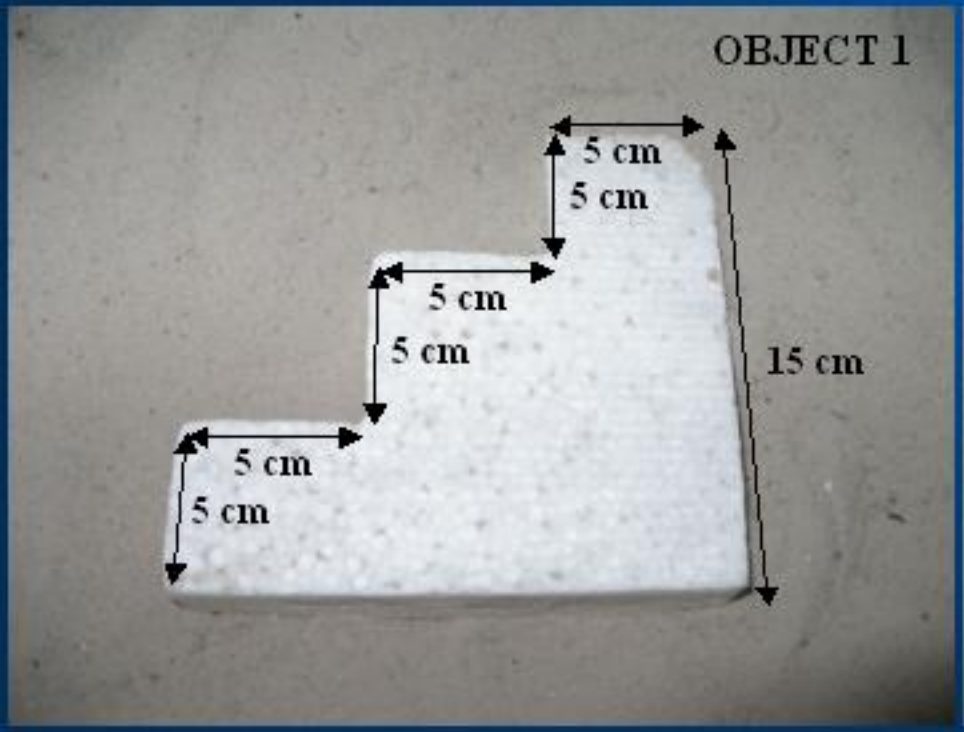

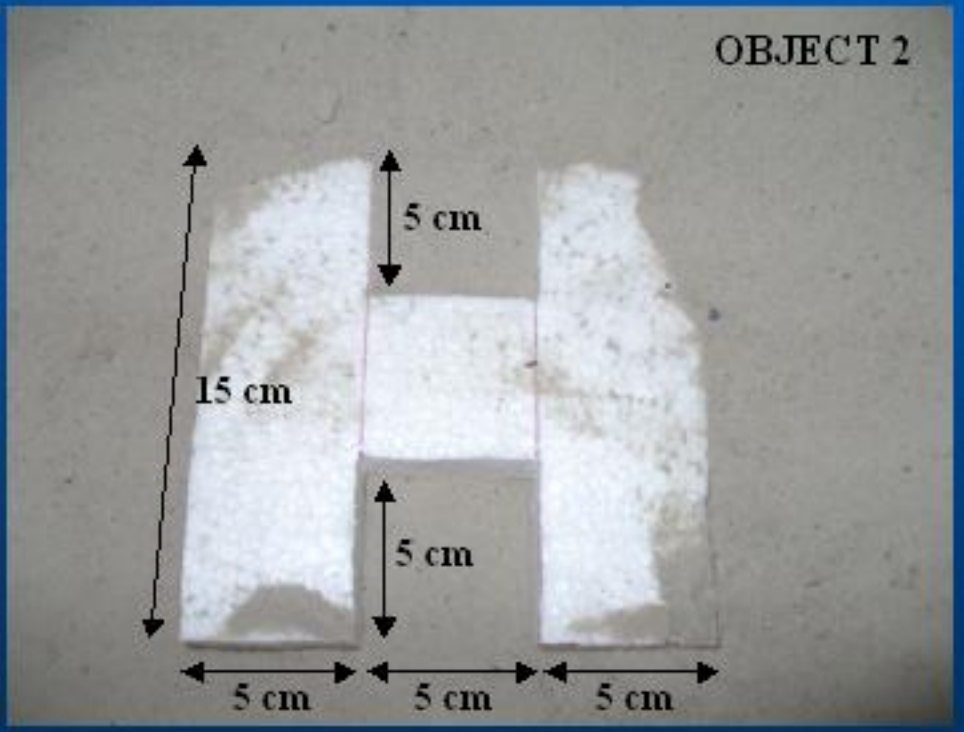

Laboratory GPR Measurements cont.

- Results for Object 1 (3-stepped foam object, depth 7 cm)
- C-Scan results without and with proper SAR processing

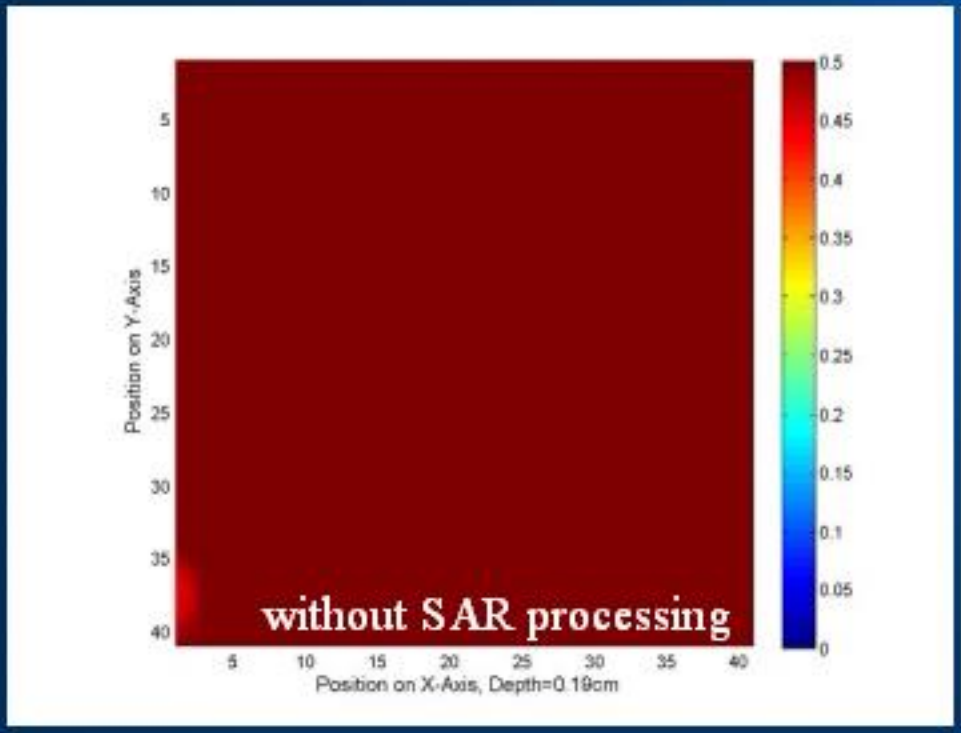

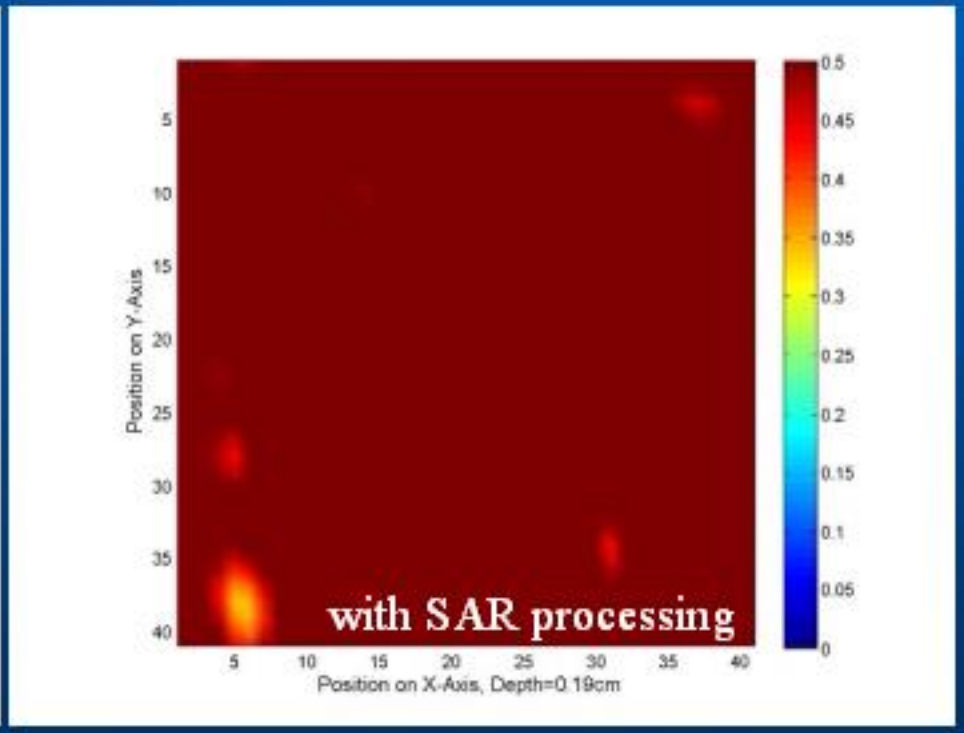

Laboratory GPR Measurements cont.

- Results for Object 2 (H-shaped foam object, depth 7 cm)
- C-Scan results without and with proper SAR processing

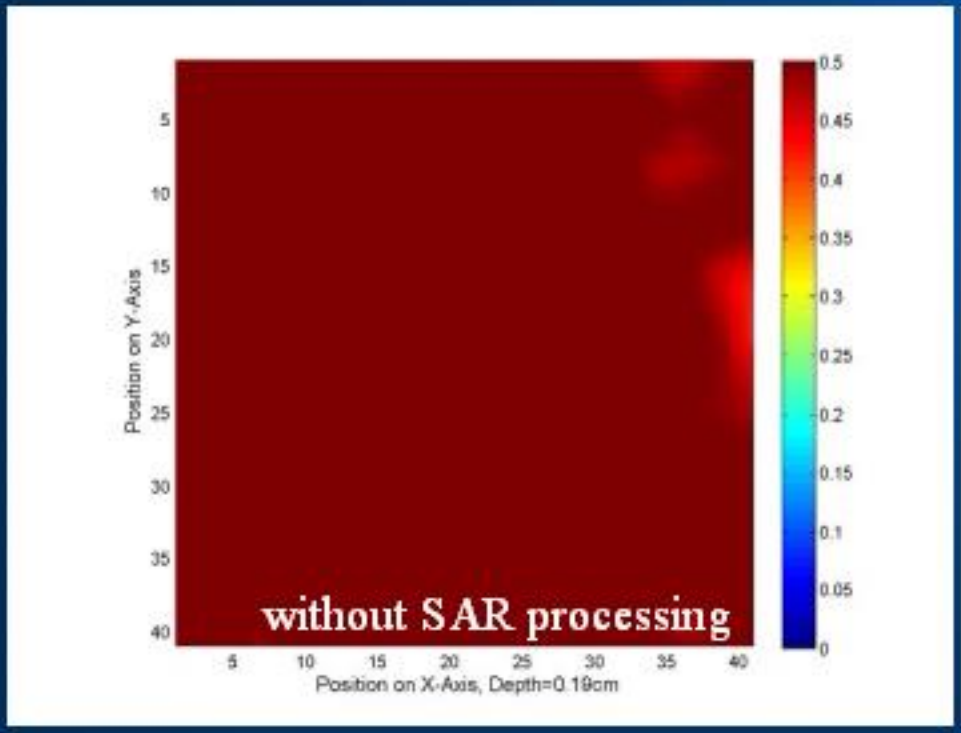

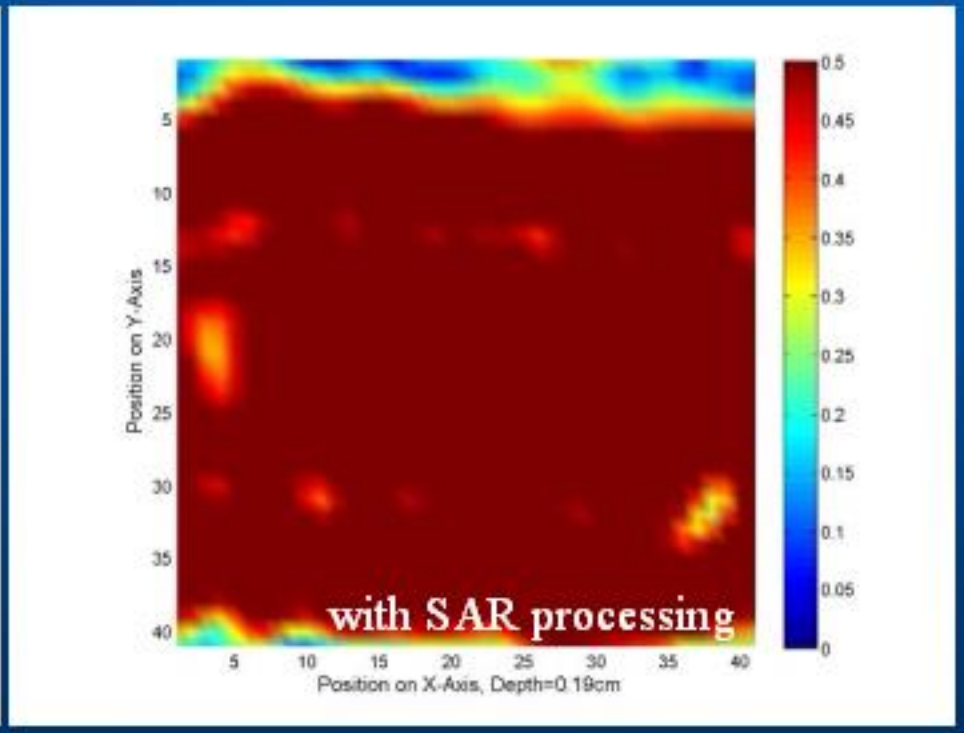

Laboratory GPR Measurements cont.

- Measurement II: TEM double-ridged horn in different heights
- VNA SFCW measurement, frequency range 3 GHz - 10 GHz

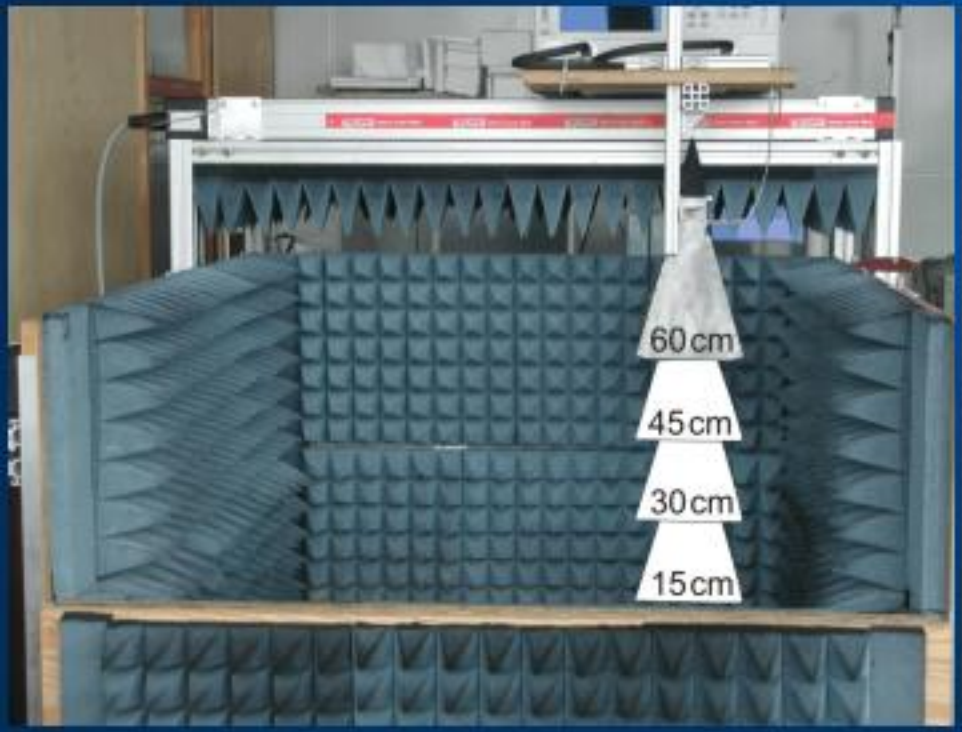

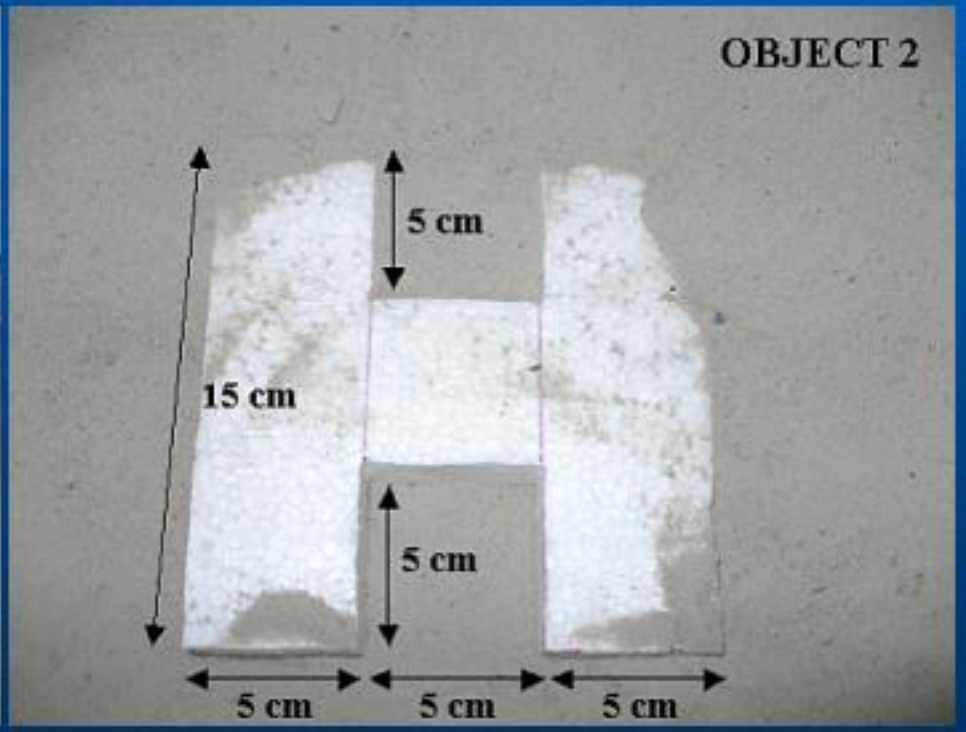

Laboratory GPR Measurements cont.

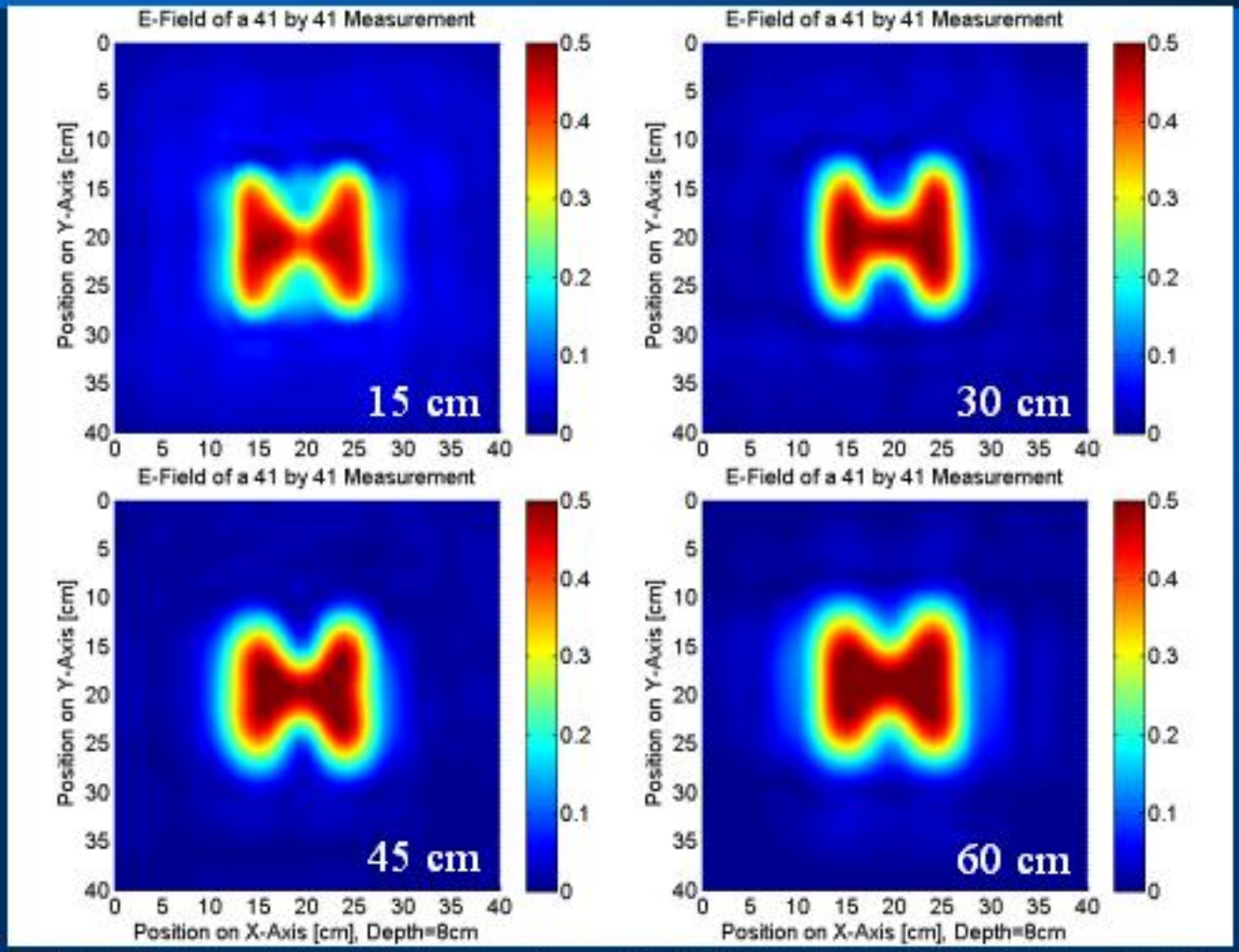

with SAR

$x_{element}=41$

$y_{element}=41$

Laboratory GPR Measurements cont.

- Measurement results for 15 cm case (left) and 60 cm case
- Only the GPR data of a 21 by 21 antenna array are utilized

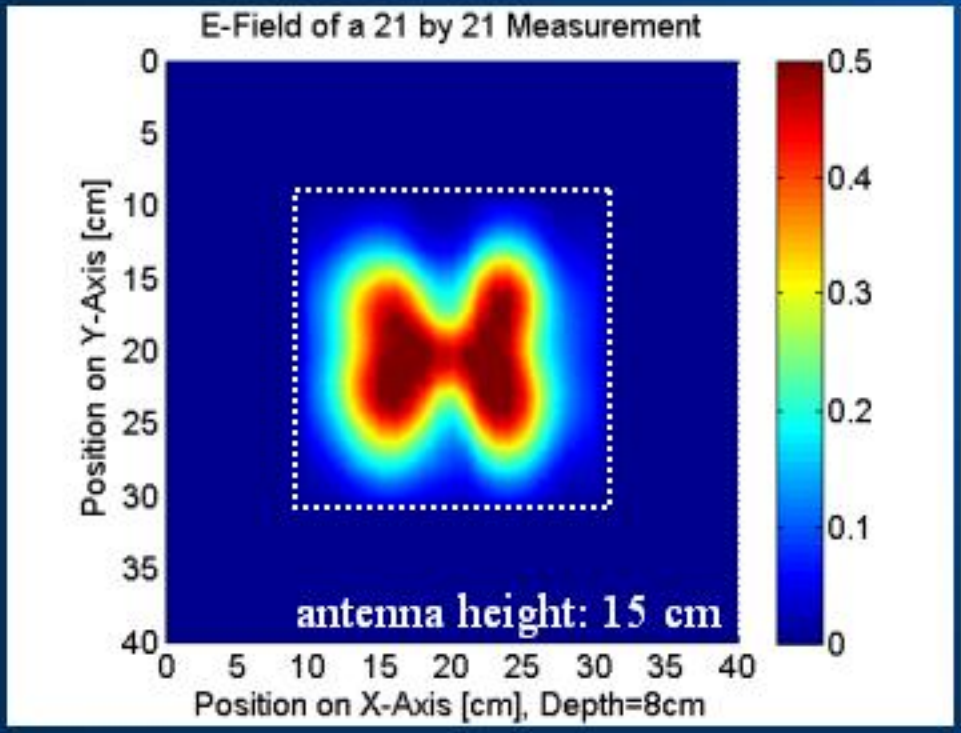

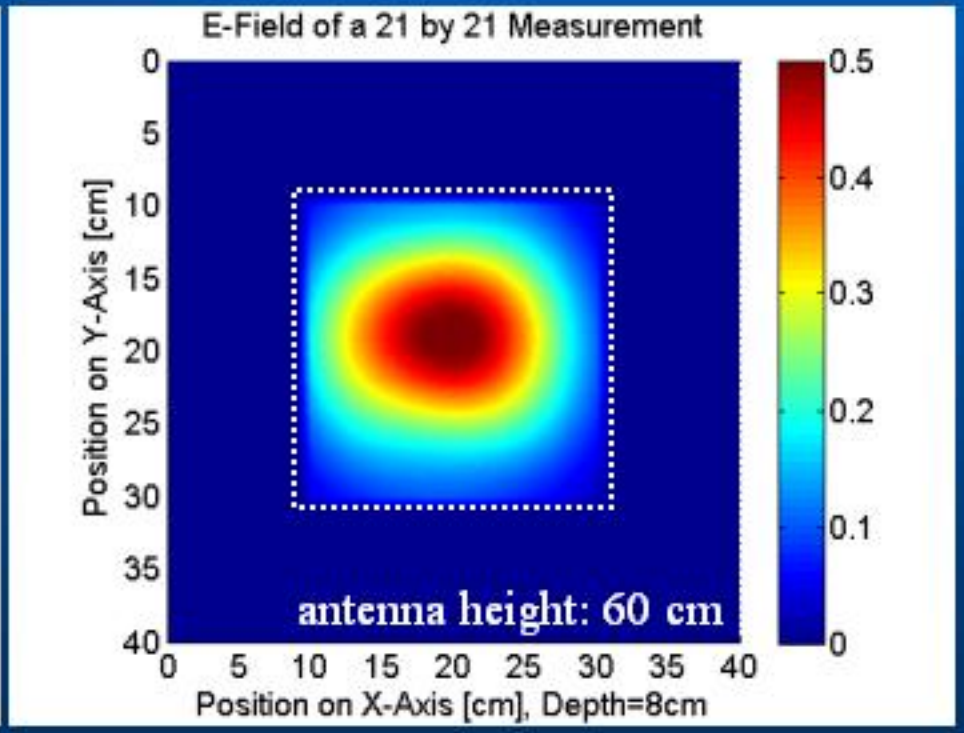

Laboratory GPR Measurements cont.

- Measurement III: TEM double-ridged horn, 2 rough surfaces
- VNA SFCW measurement, frequency range 3 GHz - 10 GHz

Laboratory GPR Measurements cont.

- Measurement results (PMN2 mine, surface wavelength 3 cm)
- Post processing: Carrier removal and background subtraction

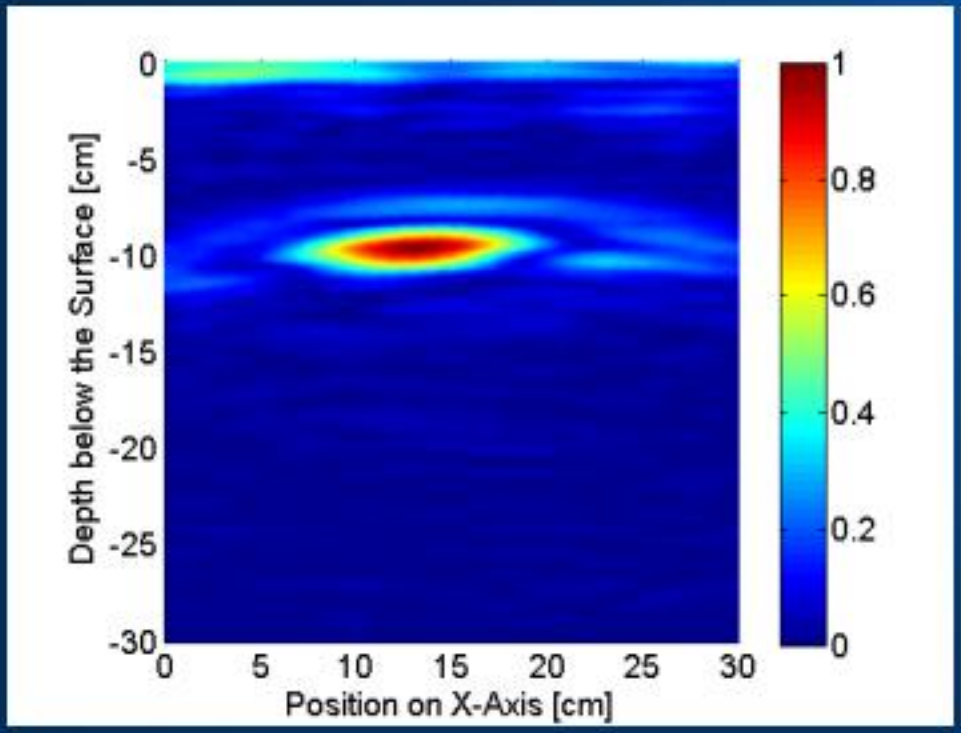

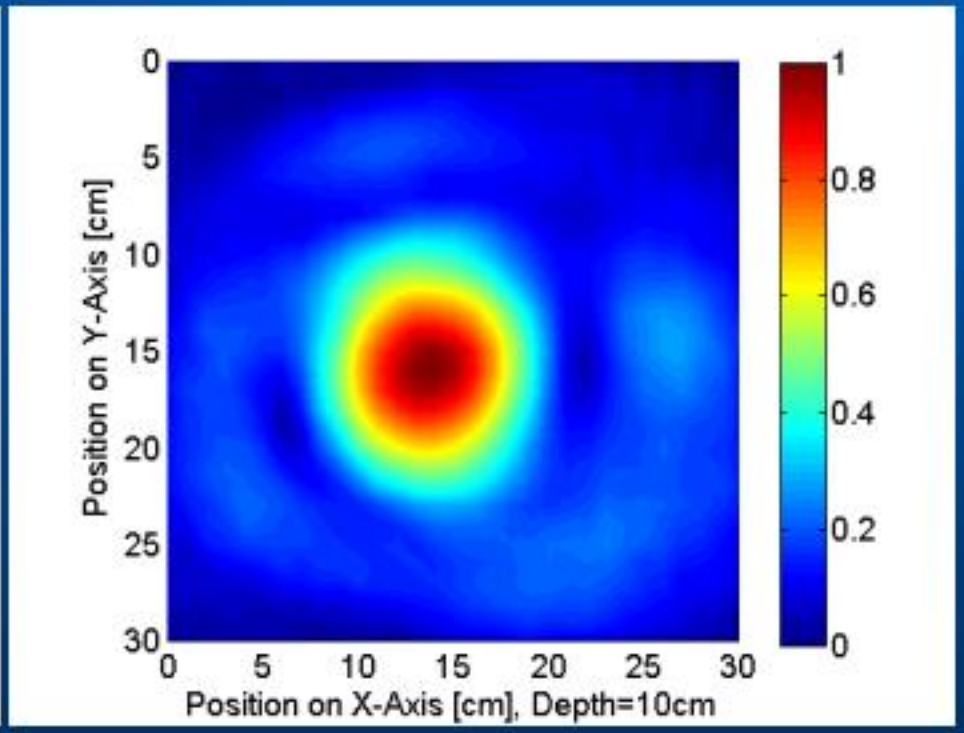

Laboratory GPR Measurements cont.

- Measurement results (PMN2 mine, surface wavelength 6 cm)
- Post processing: Carrier removal and background subtraction

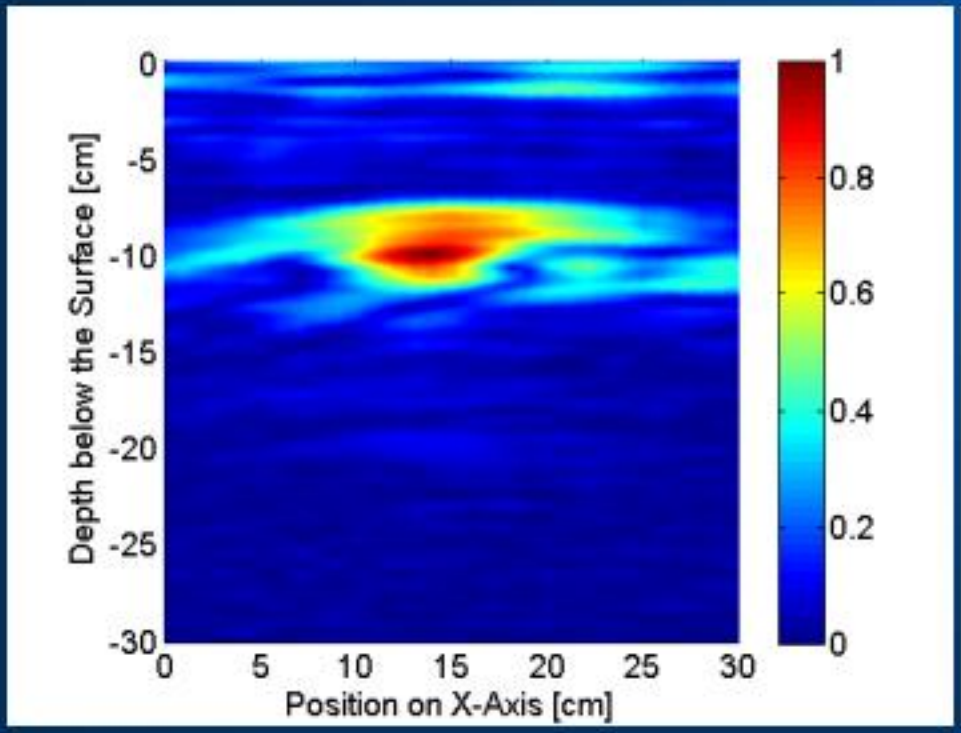

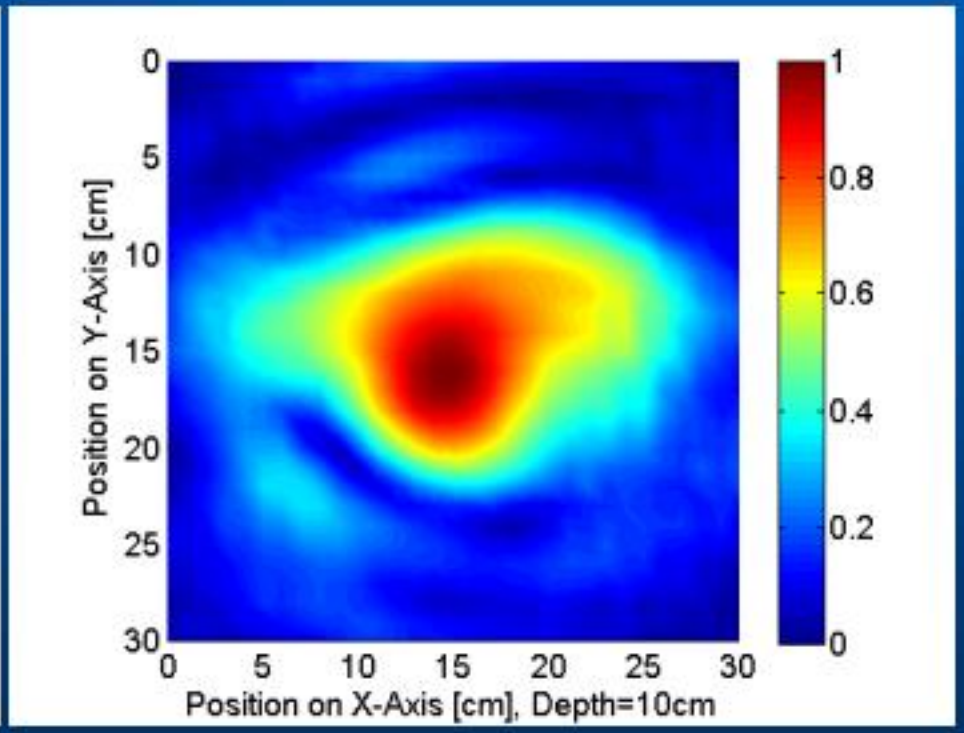

Laboratory GPR Measurements cont.

- Measurement IV: Bujanov antennas, 20 cm above the surface
- VNA SFCW measurement, frequency range 1 GHz - 16 GHz

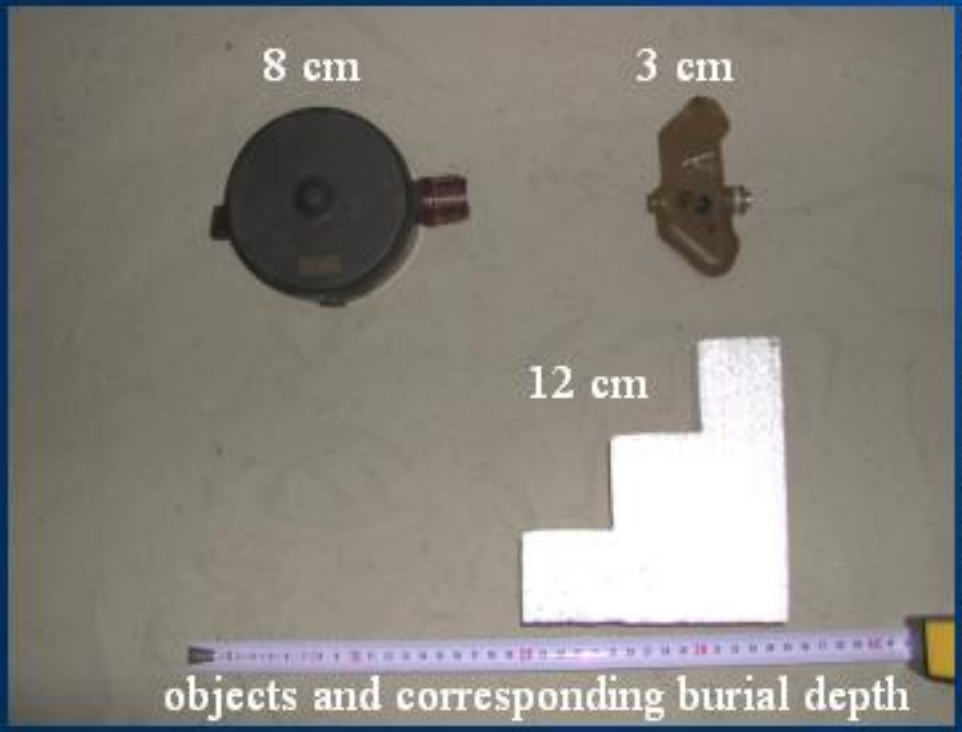

objects and corresponding burial depth


Bujanov antennas in foam

Laboratory GPR Measurements cont.

- Left hand side: Measurement results without SAR processing
- Right hand side: Measurement results with the SAR focusing

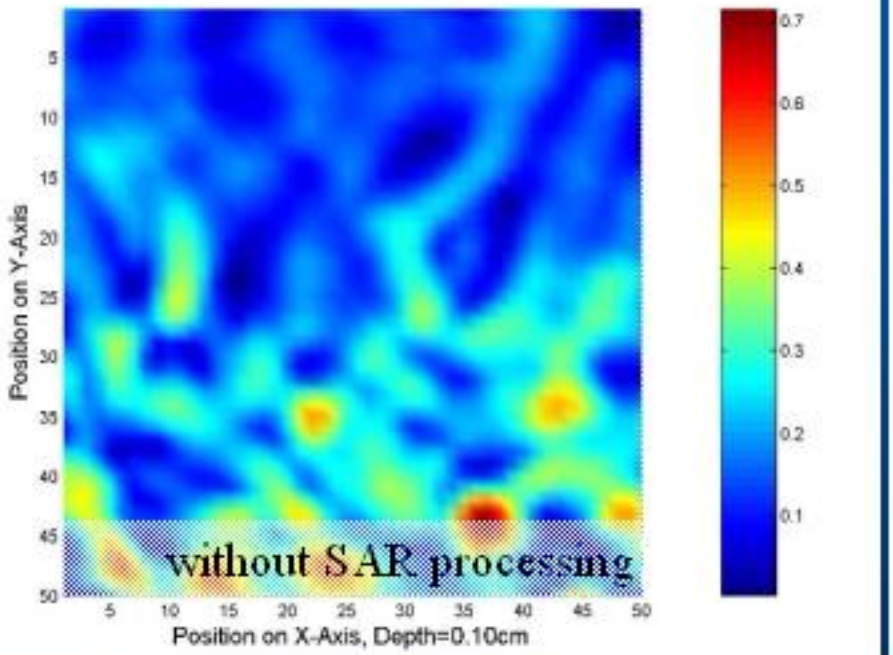

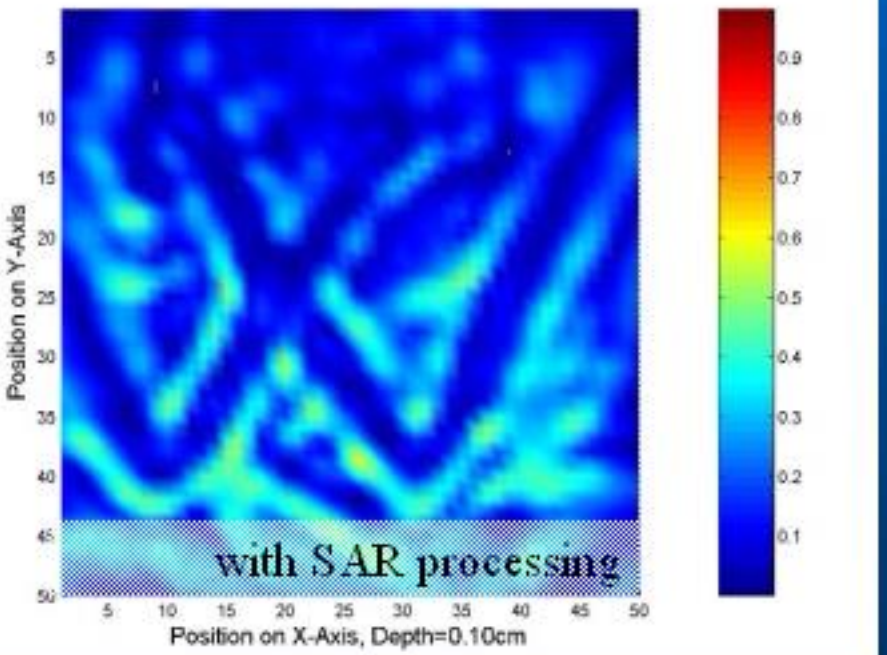

Laboratory GPR Measurements cont.

- All resulting C-Scan images have been combined to one
- Target objects can be easily detected at correct positions

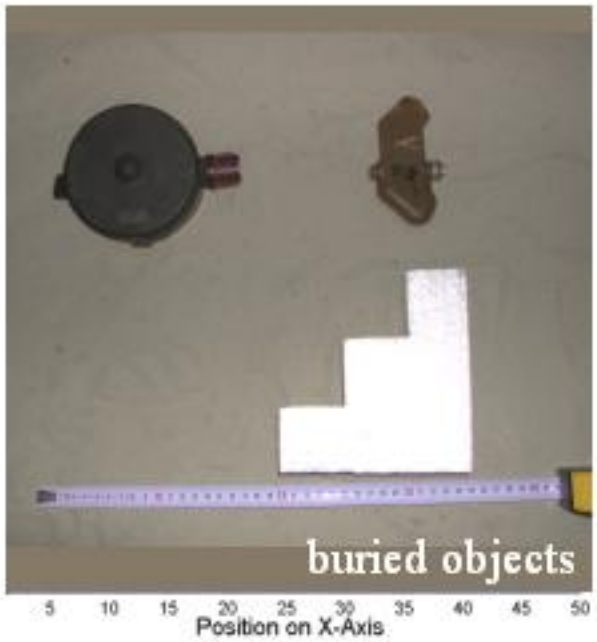

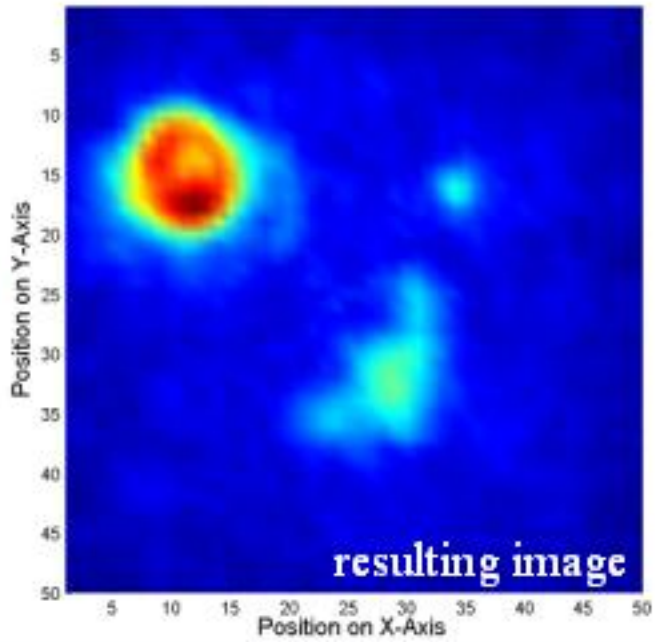

Laboratory GPR Measurements cont.

- Measurement V: 10 dB standard gain horn antenna (Ka-band)
- VNA SFCW measurement, frequency range 26 GHz - 40 GHz

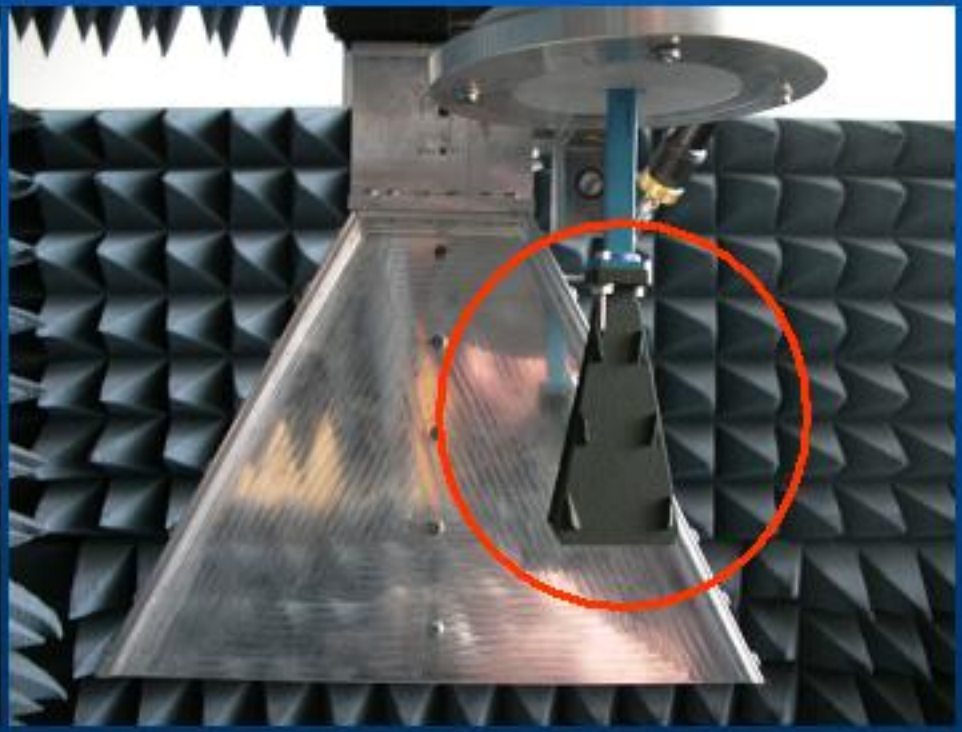

Outdoor GPR Measurements cont.

- Measurement results for M14 mine (left) and metal cylinder
- Object diameter 5 cm, object depth 16 cm below the surface

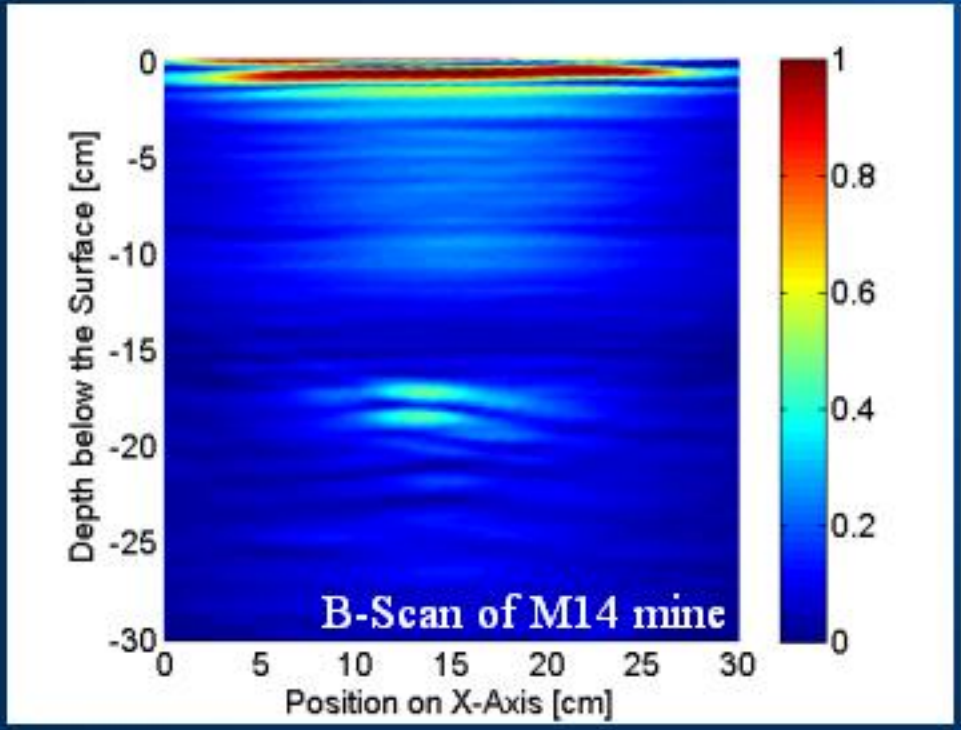

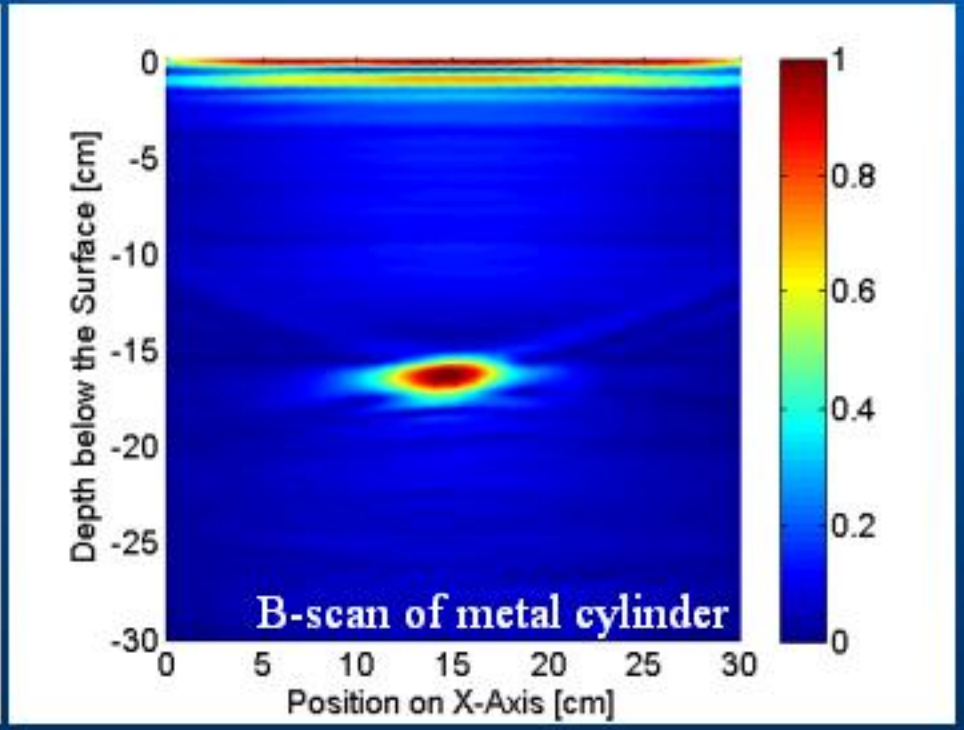

Laboratory GPR Measurements cont.

- C-Scan measurement with 41 by 51 different positions
- Width of the lines at the surface of the soil is only 2 cm

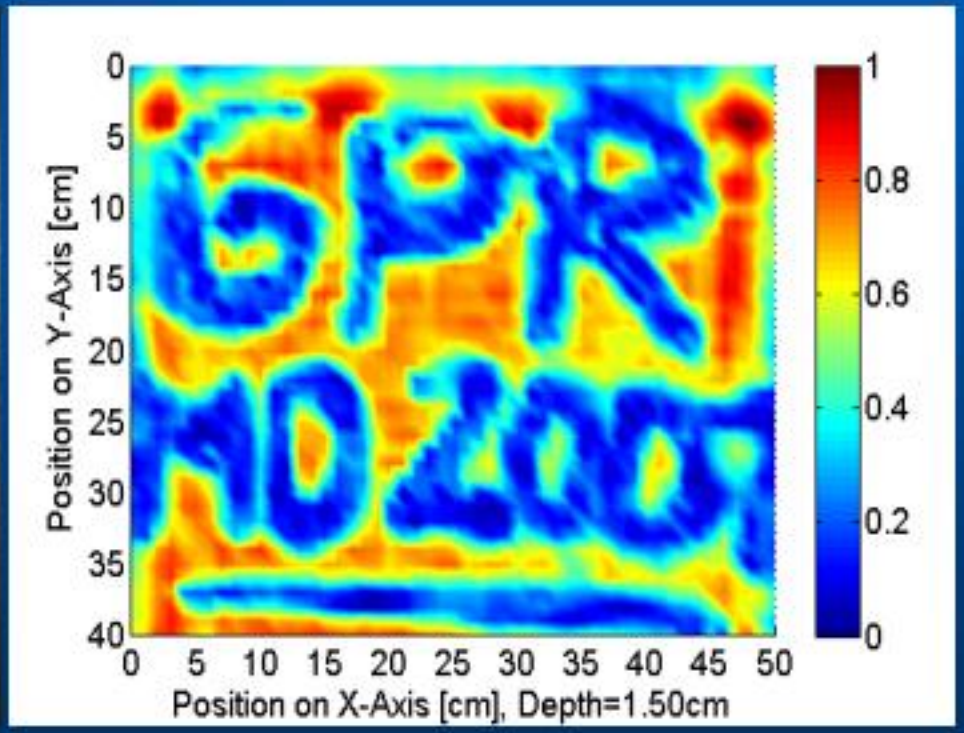

Laboratory GPR Measurements cont.

- Measurement VI: 20 dB standard gain horn antenna with lens
- VNA SFCW measurement, frequency range 8 GHz - 12 GHz

Laboratory GPR Measurements cont.

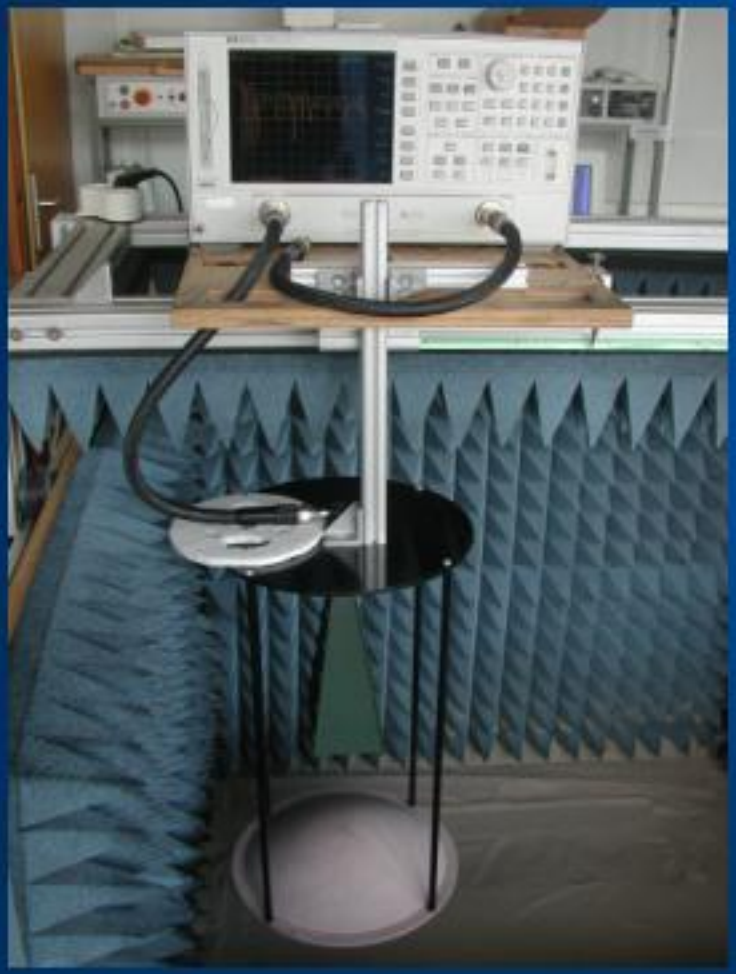

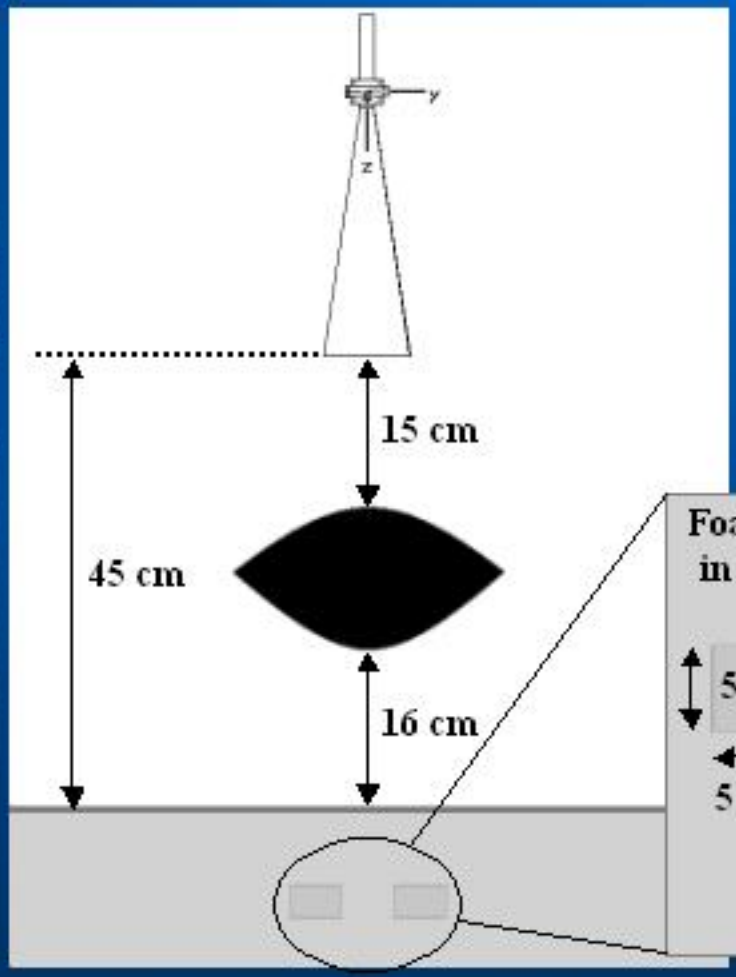

Laboratory GPR Measurements cont.

- Results of a 20 dB standard gain horn without and with lens
- Post processing: Carrier removal and background subtraction

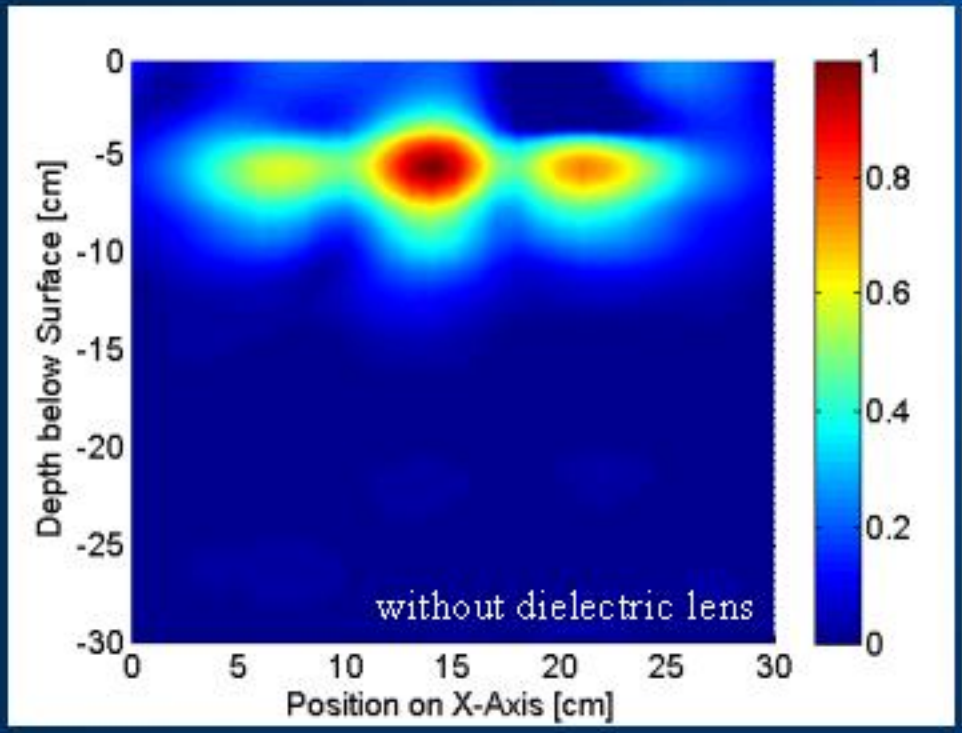

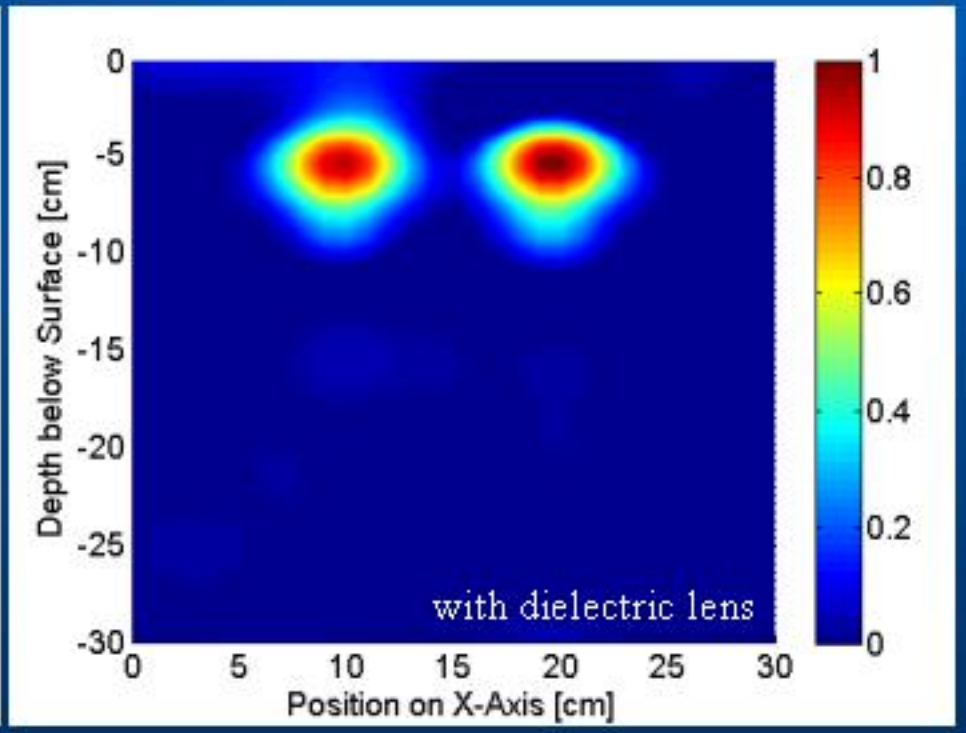

Outline

- Introduction
- 3D Field Simulation of a GPR
- SAR Focusing Techniques for GPR
- Laboratory GPR Measurements
- Outdoor GPR Measurements
- Conclusion

Outdoor GPR Measurements

Outdoor GPR Measurements cont.

- Measurement I: Indoor verification with different test objects
- VNA SFCW measurement, frequency range 1.5 GHz - 6 GHz

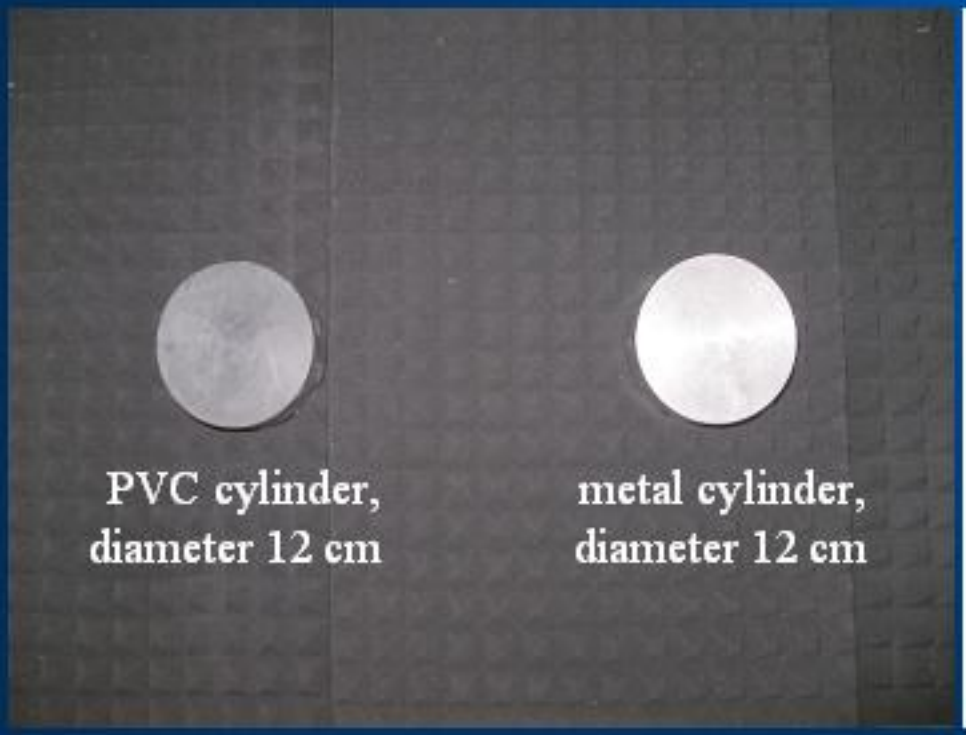

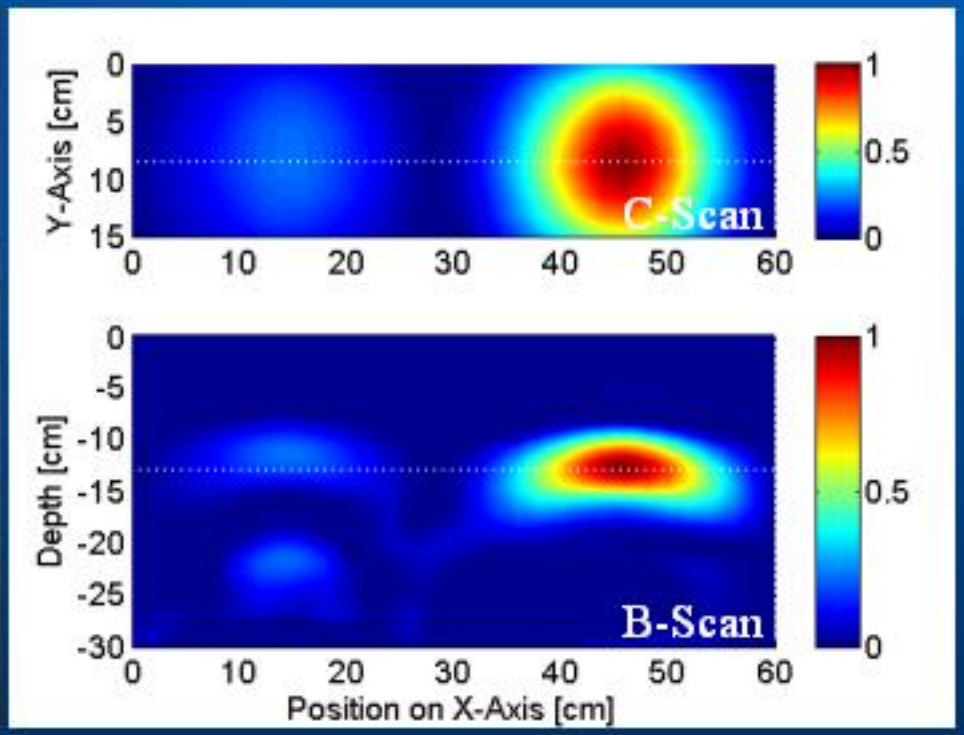

Outdoor GPR Measurements cont.

- Measurement II: Indoor verification with anti-personnel mines
- VNA SFCW measurement, frequency range 1.5 GHz - 6 GHz

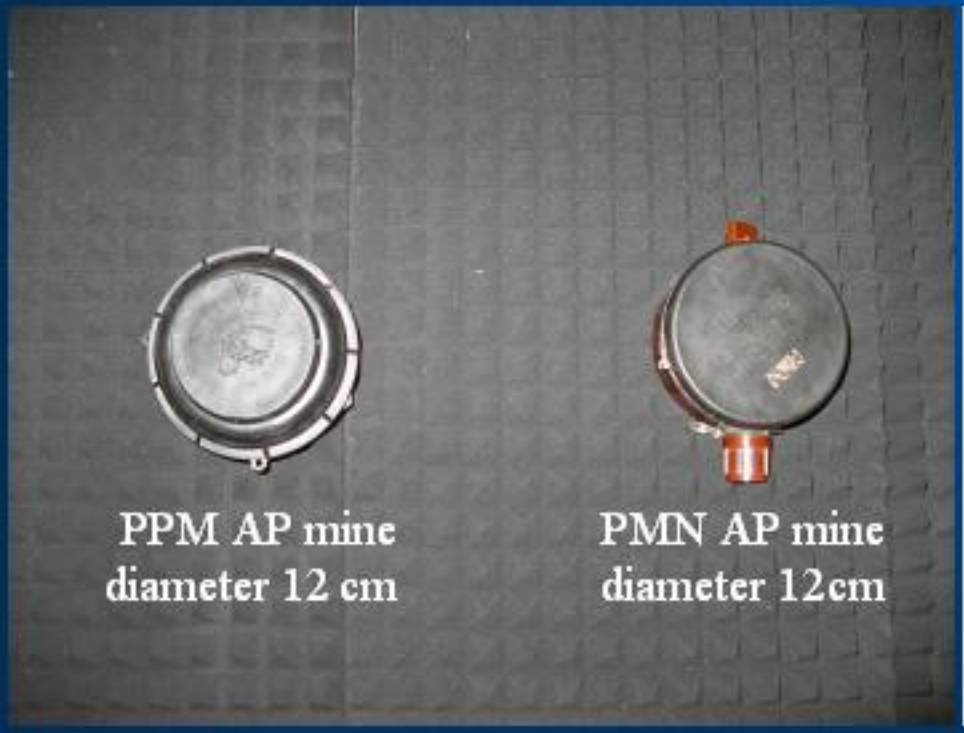

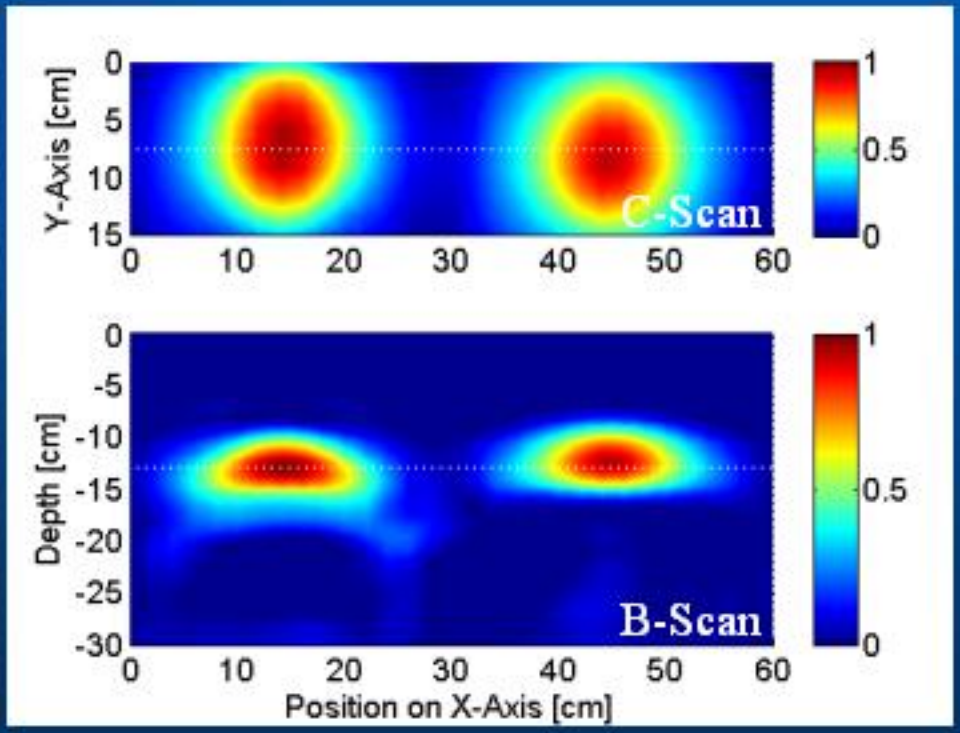

Outdoor GPR Measurements cont.

- Measurement III: Outdoor detection of buried AP landmines
- VNA SFCW measurement, frequency range 1.5 GHz - 6 GHz

Outdoor GPR Measurements cont.

- PMN AP-Mine (diameter 12 cm, buried in a depth of 6 cm)
- FSH6 C-Scan measurement: frequency range 1 GHz - 6 GHz

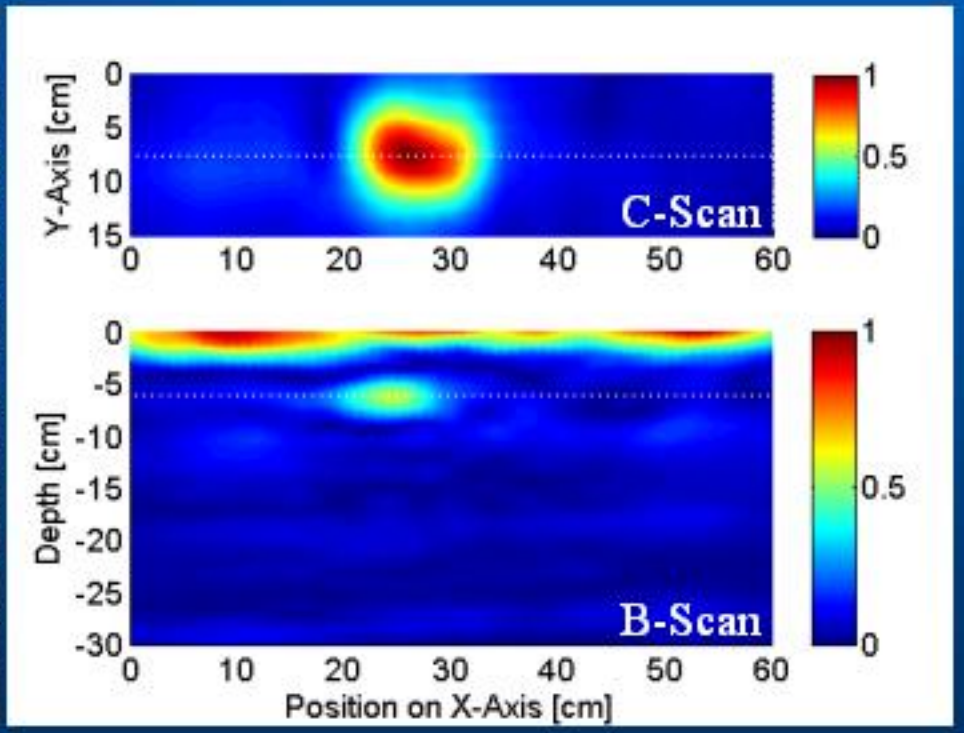

Outdoor GPR Measurements cont.

- PPM AP-Mine (diameter 12 cm, buried in a depth of 6 cm)
- FSH6 C-Scan measurement: frequency range 1 GHz - 6 GHz

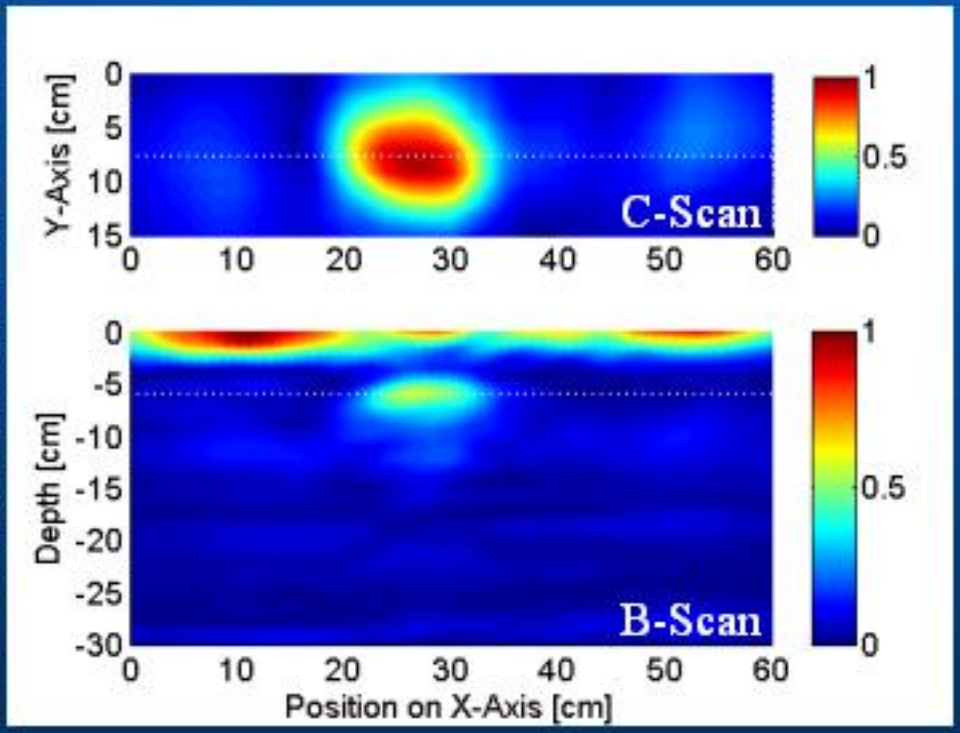

Outline

- Introduction
- 3D Field Simulation of a GPR
- SAR Focusing Techniques for GPR
- Laboratory GPR Measurements
- Outdoor GPR Measurements
- Conclusion

Conclusion

- Advanced 3D EM field simulation of a GPR
- Application of SAR focusing concept for GPR
- Determination of the influence of different array parameter on the quality of the SAR processing
- Experimental GPR setups for laboratory/outdoor measurements have been developed and verified
- Systematic investigation of different parameter
- Verification of the SAR focusing for a GPR

Thank you for your attention! - Questions?

Otto-von-Guericke-University of Magdeburg, FEIT
Electronics, Signal Processing and Communications
alexander.teggatz@e-technik.uni-magdeburg.de